Global Change Biology (2001) **7,** 755–777

Carbon storage and fluxes in ponderosa pine forests at different developmental stages

B.E.LAW,* P.E.THORNTON,† J.IRVINE,* P.M.ANTHONI‡ and S.VAN TUYL*
College of Forestry, Oregon State University, Corvallis, OR 97331, USA, †School of Forestry, University of Montana, Missoula, Montana, 59812, USA, ‡College of Oceanic and Atmospheric Sciences, Oregon State University, Corvallis, OR 97331, USA

Abstract

We compared carbon storage and fluxes in young and old ponderosa pine stands in Oregon, including plant and soil storage, net primary productivity, respiration fluxes, eddy flux estimates of net ecosystem exchange (*NEE*), and Biome-BGC simulations of fluxes. The young forest (Y site) was previously an old-growth ponderosa pine forest that had been clearcut in 1978, and the old forest (O site), which has never been logged, consists of two primary age classes (50 and 250 years old). Total ecosystem carbon content (vegetation, detritus and soil) of the O forest was about twice that of the Y site (21 vs. 10 kg C m^{-2} ground), and significantly more of the total is stored in living vegetation at the O site (61% vs. 15%). Ecosystem respiration (R_e) was higher at the O site (1014 vs. 835 g C m^{-2} $year^{-1}$), and it was largely from soils at both sites (77% of R_e). The biological data show that above-ground net primary productivity (*ANPP*), *NPP* and net ecosystem production (*NEP*) were greater at the O site than the Y site. Monte Carlo estimates of *NEP* show that the young site is a source of CO_2 to the atmosphere, and is significantly lower than *NEP*(O) by *c.* 100 g C m^{-2} $year^{-1}$. Eddy covariance measurements also show that the O site was a stronger sink for CO_2 than the Y site. Across a 15-km swath in the region, *ANPP* ranged from 76 g C m^{-2} $year^{-1}$ at the Y site to 236 g C m^{-2} $year^{-1}$ (overall mean 158 ± 14 g C m^{-2} $year^{-1}$). The lowest *ANPP* values were for the youngest and oldest stands, but there was a large range of *ANPP* for mature stands. Carbon, water and nitrogen cycle simulations with the Biome-BGC model suggest that disturbance type and frequency, time since disturbance, age-dependent changes in below-ground allocation, and increasing atmospheric concentration of CO_2 all exert significant control on the net ecosystem exchange of carbon at the two sites. Model estimates of major carbon flux components agree with budget-based observations to within ± 20%, with larger differences for *NEP* and for several storage terms. Simulations showed the period of regrowth required to replace carbon lost during and after a stand-replacing fire (O) or a clearcut (Y) to be between 50 and 100 years. In both cases, simulations showed a shift from net carbon source to net sink (on an annual basis) 10–20 years after disturbance. These results suggest that the net ecosystem production of young stands may be low because heterotrophic respiration, particularly from soils, is higher than the NPP of the regrowth. The amount of carbon stored in long-term pools (biomass and soils) in addition to short-term fluxes has important implications for management of forests in the Pacific North-west for carbon sequestration.

Keywords: carbon cycle, eddy covariance, ponderosa pine, Oregon, productivity, net ecosystem exchange, biomass, soil carbon, ecosystem process model

Received 23 November 2000; revised version received and accepted 18 April 2001

Correspondence: Beverly Law, 328 Richardson Hall, College of Forestry, Oregon State University, Corvallis, OR 97331-5752, USA, tel. +1 541-737-6111, e-mail lawb@fsl.orst.edu

Introduction

The dynamics of the terrestrial biosphere in response to environment is an integral part of understanding consequences of global change. It is important to quantify carbon storage and fluxes in different vegetation types and developmental stages, and analyse mechanisms involved in carbon cycling to better monitor the processes that regulate the uptake, storage and release of CO_2 by terrestrial ecosystems.

Carbon storage and exchange with the atmosphere is influenced by climate, physiological differences in vegetation associated with age and functional group, soil heterotrophs, and disturbance effects (e.g. logging, fire and time since disturbance). Studies suggest that net ecosystem production decreases in young stands because decomposition of dead biomass from the previous forest generation results in respiration that is higher than the NPP of the regrowth. In a boreal forest, it takes decades for NPP to exceed heterotrophic respiration (Schulze *et al*. 2000). It can take anywhere from 2 to 5 years in the South-east U.S. for young regenerating coniferous forests to become a net carbon sink (H. L. Gholz, personal communication) following clearcutting, and *c.* 20–30 years in Pacific North-west conifers (Cohen *et al*. 1996). Although this has implications for management of forests in terms of C sequestration, there is much uncertainty in these estimates because of variation in age, management and climate, and lack of measurements across a range of conditions within forest type.

The role of forests in the global carbon cycle is quantified by the net ecosystem exchange of carbon between forests and the atmosphere (NEE), which is the difference between two large fluxes, photosynthesis and respiration by autotrophs (R_a) and heterotrophs (R_h). NEE is also described as the balance between net primary productivity (NPP) and R_h. NEE can be quantified seasonally and annually from micrometeorological measurements using the eddy covariance method. These measurements, combined with modelling and measurements of respiration, photosynthesis, and carbon storage, can help us to better understand how ecosystem processes are influenced by climate, age, and management, and how seasonal dynamics affect annual carbon balances. A mechanistic understanding allows us to provide insights on how management practices can be modified to improve C sequestration across landscapes and forest types.

We conducted ecological and micrometeorological measurements in young and old ponderosa pine forests in Central Oregon. Ponderosa pine forests are the most widely distributed pine in North America (USDA 1965), and account for 22% of western U.S. timberland (Powell *et al*. 1993). Thus, it is an important forest type in which to quantify carbon cycling. In our study area, ponderosa pine occupies a 30–40 km wide band east of the Cascade Mountains, where the forests transition from a more mesic habitat of fir species into ponderosa pine and then juniper woodlands to the east, because of drier conditions. The sites are part of the AmeriFlux network of sites that is presently measuring CO_2 and energy exchange between vegetated surfaces and the atmosphere, and measuring and modelling the component processes responsible for these exchanges. We initiated measurements at the old-growth pine site in 1996, and at the young regenerating pine site in 1998.

In this paper, we compare carbon storage and fluxes in the young and old ponderosa pine, including plant and soil storage, above- and below-ground net primary production, and respiration fluxes. We compare the above-ground production and biomass of these two sites with that of 12 plots that we measured along a 15-km transect to determine how these sites compare with the range of productivity in the region. Finally, we compare various components of carbon storage and flux measured at the sites with estimates from the current version of the Biome-BGC terrestrial ecosystem process model (Thornton 1998). The model includes processes such as phenological timing, carbon allocation to plant tissues and decomposition. We use the model results to help explain differences observed between the forests, including environmental controls on carbon exchange.

Methods and materials

Study sites

We made measurements of carbon storage and fluxes in a young ponderosa pine forest (Y site) and a relatively undisturbed old-growth forest (O site) in central Oregon in 1999 and 2000. The Y site (44°26′ N, 121°34′ W, elevation 1188 m) was previously an old-growth forest that had been clearcut in 1978, and allowed to naturally regenerate. The average age of trees in 1999, 21 years after cutting, was 15 ± 1 years old. The understorey includes manzanita (*Arctostaphylos patula*) and bitterbrush (*Purshia tridentata*). Site characteristics are summarized in Table 1. The soils are ultic haploxeralfs, and are 62% sand, 30% silt and 8% clay (Table 2).

The old-growth flux site (O site) is located in the Metolius Research Natural Area (44°30′ N, 121°37′ W, elevation 915 m). The forest has never been logged. It consists of about 27% old trees (*c.* 250 years old), 25% younger trees (*c.* 50 years old) and 48% mixed-age trees. The understorey is sparse with patches of bitterbrush, bracken fern (*Pteridium aquilinum*) and strawberry

(*Fragaria vesca*). The soils are alfic vitrixerands, and texture (65% sand, 25% silt and 10% clay) is similar to that of the Y site.

Along a 15-km swath from the Cascade Mountains eastward, we measured above-ground biomass, net primary productivity and leaf area index (LAI) to characterize the range of conditions that exist for ponderosa pine in this region (Fig. 1).

Most of the precipitation in the region occurs between October and June, with the summer months lacking effective precipitation (normally 0–20 mm July through August). Winters on the east side of the Cascade Mountains are cool, and there is a large diurnal variation in temperature in summer, typical of the semi-arid region. Snow cover at the old site is intermittent, reaching a maximum depth of about 50 cm, while almost twice as much snow accumulates at the higher-altitude Y site.

Table 1 General characteristics of young (Y) and old-growth (O) pine flux sites. Height and diameter data for the O site are given for the two size classes (0–30 cm and >30 cm diameter at breast height)

	O site	Y site
Latitude	44°30′ N	44°26′ N
Longitude	121°37′ W	121°34′W
Elevation (m)	915	1188
Annual PAR (MJ m^{-2})	2369	2481
Mean Annual Temperature (°C)	8.1	7.5
Annual precipitation (mm)	524	552
Age	50/250	15
Mean height (m)	10 (0.2), 34 (0.8)	4 (0.2)
Diameter breast height (cm at 1.3 m)	12 (0.2), 63 (2.7)	6.4[1], 10 (0.5)

[1]Diameter at ground level for trees <5 cm d.b.h. (used in allometrics for estimating biomass, ANPP of small ponderosa pine trees)

Environmental measurements

We made micrometeorological measurements and used the eddy covariance method to determine half-hourly fluxes of CO_2 and water vapour above the forest canopy at the O site (47 m height, 14 m above the canopy) and Y site (20 m height, 16 m above the canopy). Wind speed and temperature were measured with a three-dimensional sonic anemometer (Solent model 1012 R2, Gill instruments, Lymington, England; CSAT-3 Campbell Scientific, Inc, Utah), and water vapour and CO_2 fluctuations were measured with open-path infrared gas analysers (Li-7500, LI-COR Inc, Lincoln, NE; NOAA ATDD, Oak Ridge, TN, Auble & Meyers 1992) that respond to frequencies up to 15 Hz. Details on the instrumentation, flux correction methods and calculations were reported in Law *et al*. (1999a,b) and Anthoni *et al*. (1999). We summarize methods here to briefly explain processing of the flux data.

The CO_2 and water vapour fluxes were corrected for density fluctuations arising from variations in temperature and humidity (Webb *et al*. 1980) and for influences of horizontal wind speed on virtual temperature (Schotanus *et al*. 1983). The data were screened to remove possible eddy covariance instrumentation and sampling problems (Law *et al*. 1999a). Fluxes were also rejected when inconsistently large CO_2 fluxes were observed. Data gaps were filled based on an empirical relationship with environmental variables where Michaelis–Menten model parameters were determined seasonally from valid flux data from surrounding days (Anthoni *et al*. 1999). During turbulent conditions, the change in CO_2 storage, determined from profile measurements in the canopy airspace, was combined with above-canopy flux measurements to estimate NEE. Calm periods lead to accumulation of CO_2 in the area and to a large change in storage in the early morning hours. During those conditions the carbon exchange was modelled from functional relationships with radiation and vapour pressure deficit when more turbulent conditions existed (Anthoni *et al*. 1999).

Table 2 Soil chemistry, where first value is for the young pine site (Y) and the second value is for the old forest (O)

Depth	Site	Bulk density	Total C (kg m^{-2})	Total N (kg m^{-2})	Soil texture (% sand, silt, clay)
0–20 cm	Y	1.18	2.62	0.171	69, 26, 5
	O	1.05	2.79	0.104	65, 25, 10
20–50 cm	Y	1.44	0.84	0.157	63, 30, 7
	O	1.15	1.65	0.091	67, 23, 10
50–100 cm	Y	1.42	0.86	0.175	54, 35, 11
	O	1.23	1.44	0.132	63, 26, 11
Total	Y		4.31	0.50	62, 30, 8
	O		5.87	0.33	65, 25, 10

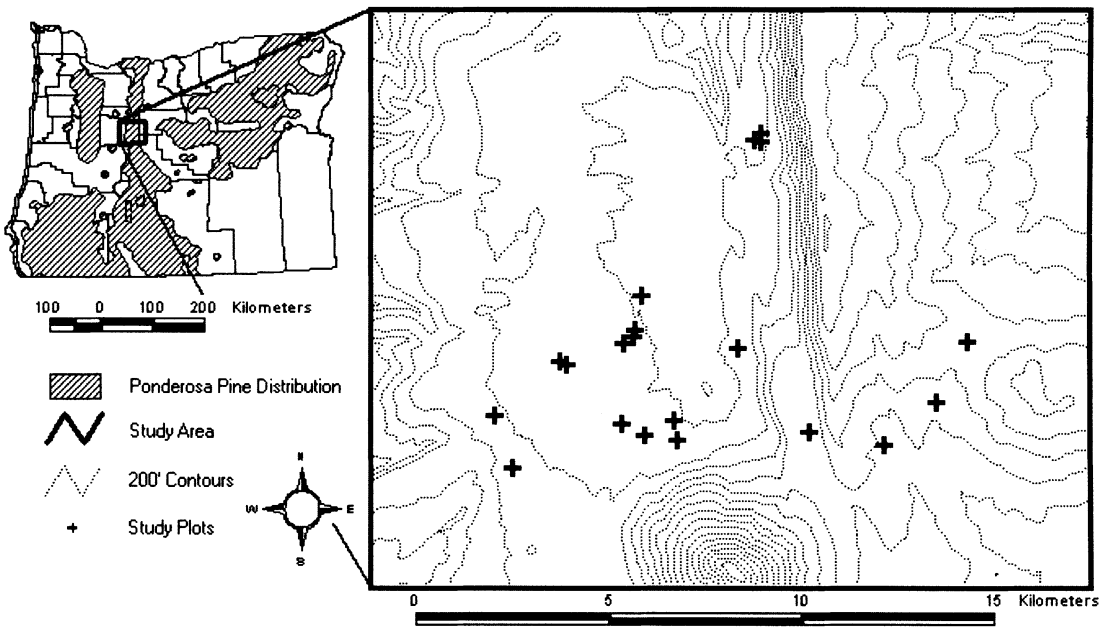

Fig. 1 Location of flux sites and transect of pine plots in Central Oregon.

Half-hourly measurements of climatic variables made at the top of the flux towers included air temperature (T_{air}), vapour pressure deficit (D), incident photosynthetically active radiation (PAR), and rainfall. Seasonal climate summaries are shown in Fig. 2. Soil moisture was measured at 10 and 30 cm depths horizontally (CS615s, Campbell Scientific, Logan, UT) and soil temperatures (T_s) at 2, 8 and 15 cm depth were recorded in six locations. Manual measurements of soil moisture were also made periodically across the sites by time domain reflectometry over 0–30 cm and 0–80 cm depth (Tektronix, Beaverton, OR).

Carbon budgets from biological measurements

We made measurements on above- and below-ground live plant tissue, coarse and fine woody detritus and litterfall to investigate differences in annual carbon storage and fluxes between sites. We also measured photosynthesis and predawn water potential seasonally to investigate differences in water limitations to carbon uptake in trees.

Leaf area index

We established 100 × 100 m plots for measurements of leaf area index (LAI), biomass and NPP. Three of the plots were at the O site; one in a pure old-growth stand, one in a 50-year-old stand, and one in a mixed stand. All three plots were within 200 m of the flux tower. At the Y site, the flux tower was located *c.* 40 m south-west of the plot centre. As part of another project, we measured canopy structure and LAI at 12 additional plots in ponderosa pine along an east–west swath that included the western extent of the species near the Cascade Mountains, with the Y site at the eastern end of the swath. The information was used to explain the range of ANPP expected in this region, and to test the representativeness of the flux sites.

Leaf area index was determined from optical measurements with a LAI-2000 (LICOR, Lincoln, NE) on a 10-m grid on each 100 × 100 m plot. Measurements were made in diffuse sky conditions (twilight). LAI (one-half total leaf surface area per m^2 ground area) was corrected for foliage clumping within shoot, clumping at scales larger than shoot, and wood interception of light (Chen 1996; Law *et al*. 2001a; Law *et al*. 2001b). Clumping within shoots was determined in Law *et al*. (2001a). Clumping at scales larger than the shoot was computed from measurements with a TRAC instrument along two 100-m transects at each plot (TRAC, 3rd Wave Engineering, Ontario, Canada). The canopy structure data were used to correct LAI measurements for wood interception of light.

Above-ground biomass and productivity

Five 10-m radius subplots were established within each of the plots for structure measurements. GPS coordinates were obtained for the subplot centres. Tree height, height to base of live crown and diameter breast height (d.b.h. at 1.3 m) were measured on all trees

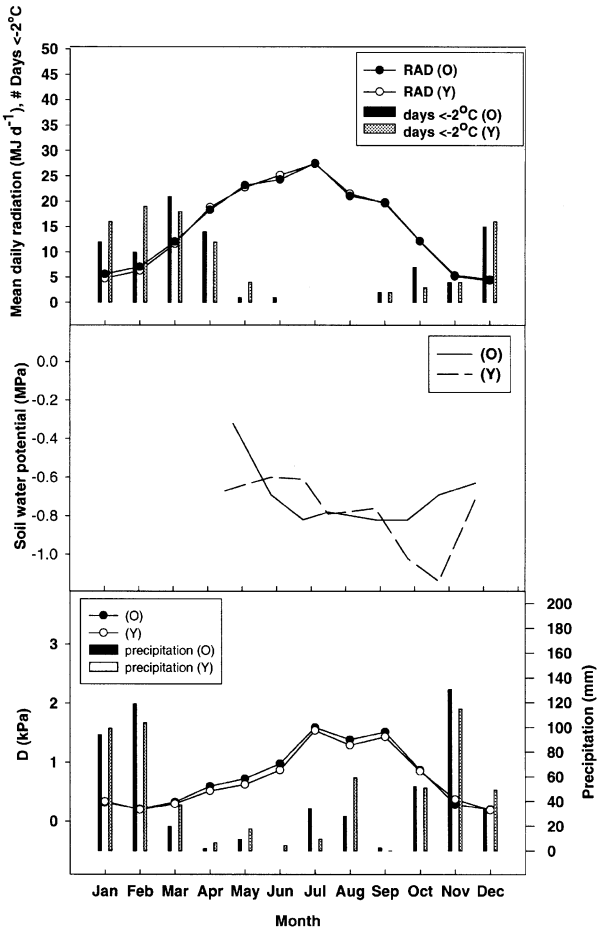

Fig. 2 The climate at the Y *and* O sites in 1999 was similar, although annual precipitation and radiation were slightly higher at the Y site. Data include (a) total solar radiation and number of days per month with freezing temperatures, (b) soil water potential, estimated from pre-dawn leaf water potential by accounting for the gravitational effect, and (c) monthly mean daytime vapour pressure deficit (D) and monthly summed precipitation.

greater than 5 cm d.b.h., and the smaller trees were tallied. All trees were measured on the old-growth plot at the O site. Tree height and base of live crown were measured with a laser ranging scope (MapStar and Impulse 200, Laser Tech, Inc., Englewood, CO). At the Y site, dimensions were measured on all trees (height, diameter at tree base, base of crown and d.b.h.), and shrubs (length, width, height and diameter at shrub base) on the subplots. Wood cores from three trees per subplot were taken to determine growth increment, wood density and age. Above-ground biomass of stems and bark for trees >5 cm d.b.h. was determined from allometric equations developed at the O site (S. Acker, personal communication), and branch mass was determined from Gholz (1982; Table 3). Above-ground biomass for trees <5 cm d.b.h. at the O site was determined from allometrics developed in pine stands in south-central Oregon (Ross & Walstad 1986). At the Y site, we developed our own allometric equations from destructive harvest of five trees representing the range of sizes present (Table 3). ANPP of woody tissue was calculated from change in biomass, using the 1-year growth increment data for previous d.b.h. measurements of trees. Shrub biomass and NPP were determined from destructive harvest of five to nine shrubs per species at the Y site, and scaled to site by number of shrubs per size class.

Foliage turnover rate (28%) was estimated from the fraction of total dry mass of foliage on 10 shoots that had fully expanded. Foliage samples were collected from the top, middle and lower canopy to determine mean leaf mass per unit leaf area (LMA, g C m^{-2} leaf). Tree foliage biomass was determined from LAI and LMA, and tree foliage production was calculated from foliage biomass, and turnover rate. We also used the mean of 2 years of litterfall data as a second estimate of foliage production. Ponderosa pine carries 3 years of foliage in this area, so the 2-year mean is likely to be less affected by interannual climate effects on production than using only 1 year of data.

Litterfall production

Litterfall production (< 1 cm diameter) was determined from 1 year of monthly collections of litterfall in 20 trays (0.13 m^2 each) at both sites. Litter was separated into foliage and woody material, dried at 70 °C for 48 h, then weighed. Fresh leaf litter C content was 50%. Forest floor litter biomass was estimated from 20 10 cm diameter cores collected at both sites in June, and in this case, 52% of litter mass was carbon (includes older litter).

Below-ground biomass and productivity

Below-ground carbon allocation was determined from annual soil surface CO_2 efflux minus annual litterfall C plus coarse root production (NPP_{cr}; Giardina & Ryan 2001). Giardina and Ryan had suggested that to address possible non-steady state conditions, below-ground C allocation could be computed by including change in litterfall, soil C and NPP_{cr}, and found that NPP_{cr} was the largest contribution of the three factors, but all three were small values compared with annual soil fluxes.

Because of the difficulty in measuring fine root production, we used two methods and obtained a mean and error estimate using a Monte Carlo approach (Harmon *et al*. 2001). In the first method, total root production was estimated from below-ground C allocation minus root respiration. Coarse root mass and

Table 3 Allometric equations for estimating biomass. Allometrics were developed from destructive harvest of trees and shrubs at the young (Y) site (*Arpa* = *Arctostaphylos patula*, manzanita; *Putr* = *Purshia tridentata*, bitterbrush)

Biomass (g)	Equation	r^2	MSE	Source
Bark mass	0.067 × ht m × dbh^2 m × 345000[a] g m^{-3}			S. Acker, personal communication
Branch mass	exp((2.719 * ln(d.b.h. cm)) –5.386) * 1000			Gholz 1982
Stem mass	0.293 × ht m × dbh^2 m × 407270[b] g m^{-3}			S. Acker, personal communication
Tree mass for trees < 5 cm d.b.h.	0.150 + 0.867(exp(ln(dbh^2 cm × ht m)))			Ross & Walstad 1986
Stem mass at Y site for trees < 5 cm d.b.h.	1232.221 + 9.771(dba^{2c} cm × ht m)	0.99	1305	This study
Branch mass at Y site for trees < 5 cm d.b.h.	1577.690 + 4.646(dba^{2c} cm × ht m)	0.78	5291	This study
Stem mass at Y site for trees > 5 cm d.b.h.	4141.644 + 14.509(dbh^2 cm × ht m)	0.95	4631	This study
Branch mass at Y site for trees > 5 cm d.b.h.	2336.823 + 7.552(dbh^2 cm × ht m)	0.90	3724	This study
Arpa shrub mass	–896.869 + 1788.092(volume[d] m^3)	0.95	1116	This study
Putr shrub mass	404.459 + 241.678 (volume[d] m^3)	0.57	411	This study

[a]345000 g m^{-3} is measured bark density. [b]407270 g m^{-3} is measured wood density. [c]dba is diameter at the base of the tree; dba ranged from 2 to 26 cm. [d]Volume is measured by box dimensions of shrub (length × width × height), *Arpa* $n = 5$, *Putr* $n = 9$.

production were estimated assuming that they were 25% of above-ground wood carbon (Grier & Logan 1977), and coarse root production was subtracted from the total to get fine root production (NPP_{fr}). NPP_{fr} was also estimated from minirhizotron estimates of turnover rates and the live fine root biomass measured in the soil cores that were taken in October.

Decomposition of woody detritus, roots and litter

Coarse (> 10 cm diameter and > 1 m length) and fine (1–10 cm diameter) woody detritus biomass were measured following guidelines by Harmon & Sexton (1996). The dimensions of standing dead trees were used in the allometric equations to determine standing dead biomass, which was substantial at the O site. CO_2 fluxes from woody detritus were measured periodically in summer, before and after rain, using a LICOR 6400 and soil chamber, but not enough data were available to develop a temperature/moisture response curve. Therefore, the annual carbon loss from the coarse woody debris pool was calculated from dead biomass per m^2 ground, and a typical decomposition rate constant for ponderosa pine in this area ($k = -0.027$; M. Harmon, personal communication; Harmon *et al*. 1990). Litter decomposition rates were determined from litterbag measurements over 2 years at each site using the LIDET method (Gholz *et al*. 2000; 18% change at the O site and 14% change at the Y site).

Soil carbon distribution

Ten soil pits were dug at the O *and* Y sites, one pit every 5 m along transects with a random start. Samples were taken from 0 to 20 cm, 20–50 cm, and 50–100 cm depths. Twenty additional samples were collected from 0 to 20 cm depth at both sites. Live vegetation and roots were removed, and the total C and N were determined (Carlo-Erba C-N-S analyser), as well as bulk density and soil texture (hydrometer method, Central Analytical Laboratory, Oregon State University). Soil carbon content was calculated for each soil layer from layer depth, bulk density and percent organic carbon data, and summed for all layers to estimate total soil carbon content to 1 m.

Respiration

Foliage respiration (F_f) and soil surface CO_2 effluxes (F_s) were measured periodically through the year at both sites using chambers and a portable infrared gas analyser (LICOR 6400; LICOR, Lincoln, NE). We used equations developed at the O site to estimate woody tissue respiration from automated measurements of bole temperature (F_w; Law *et al*. 1999a). At the Y site, we used air temperature, assuming that because the tree diameters were small, air and bole temperatures were similar.

We measured foliage respiration in the dark. For the O site, we used the temperature response equation developed in Law *et al*. (1999a). Measurements were made on shrubs in addition to trees at the Y site, because they account for about one-third of the leaf area. Seasonal phenology records and maximum LAI of trees and shrubs were used to determine seasonal changes in LAI for half-hourly and annual estimates of foliage respiration.

Site-specific temperature response equations were also developed for soil surface CO_2 efflux using soil temperature measured at 8 cm depth. The temperature

response equations were used to normalize soil respiration values to a common temperature (10 °C), and the mean normalized values were interpolated between measurement dates (measurements began in March and ended in November). Half-hourly respiration was computed from automated measurements of T_{soil} for soils, T_{air} for foliage, and T_{bole} (O site) and T_{air} (Y site) for woody tissue by applying the temperature response equations. Details of the scaling methods are in Law *et al*. (1999a). We summed the half-hourly rates to estimate annual ecosystem respiration (R_e).

To determine the fraction of soil surface CO_2 efflux that was due to root respiration, we measured the total soil flux, respiration from the litter and then respiration from excised roots from within the 10 cm diameter soil collar (0–30 cm depth) at 12 locations per site. Root respiration was measured with a capped LiCor 6400 soil chamber immediately after the roots had been removed from the soil. Coarse and fine roots were measured separately. This was repeated in May, July and October. We used a linear interpolation to determine the fraction of total soil CO_2 efflux that was from roots through the year.

Net ecosystem production from biological data

The biological data were used to estimate annual NEP (NPP – R_h), where R_h was calculated from total soil surface CO_2 efflux minus root respiration, and the sum of coarse and fine woody detritus respiration. The two different estimates of fine root production, as well as two estimates of foliage production, were used in the Monte Carlo model to obtain a second calculation of NEP with an uncertainty estimate (Harmon *et al*. 2001). In the model, the values of each NEP component were varied from the mean ± 2 standard errors, assuming a normal distribution of values. The calculations were repeated 20 times and the mean and standard deviation were determined from the output.

Photosynthesis

We compared maximum carboxylation rates and predawn leaf water potential of trees at both sites across seasons to investigate differences in photosynthetic efficiency that might be linked to limitations in water availability. Assimilation rates were measured at different CO_2 concentrations ($A–C_i$ curves) in June and August, on 1-year-old foliage from mid-canopy, using a LICOR 6400 (LICOR, Lincoln, NE). Maximum carboxylation rates (V_{cmax}) were calculated from the $A–C_i$ curves using the Farquhar model fitted with parameters in De Pury & Farquhar (1997). The activation energies E_V = 68 000 J mol^{-1} and E_J = 199 000 J mol^{-1} and relations between V_{cmax} and leaf temperatures were used for normalization to 25 °C (D. Ellsworth, personal communication). Leaf water potential (ψ_p) was measured monthly (April to November) with a pressure chamber before sunrise (Scholander *et al*. 1965). These values were used to estimate soil water potential, accounting for gravitational effect (0.1 MPa per 10 m height).

Process modelling with Biome-BGC

The Biome-BGC terrestrial ecosystem process model (version 4.1.1) was implemented at the Y *and* O sites to explore possible controls on site carbon budgets and to help explain the observed differences in carbon storage and carbon fluxes between the sites. Biome-BGC is designed to simulate the dominant processes controlling fluxes of water, carbon and nitrogen in non-agricultural ecosystems (Kimball *et al*. 1997; Thornton 1998). A primary purpose of the model is to facilitate studies of net ecosystem exchange of carbon, including the influences of changing atmospheric chemistry, changing nutrient deposition rates, interannual climate variability, and natural and managed disturbances.

Daily surface weather variables are the primary model drivers, including air temperature, total precipitation, total incoming radiation, and daylight average humidity. Initial transient flux responses are avoided by performing preliminary runs in which the model state variables (especially the soil organic matter pools) are allowed to reach a steady state with respect to available surface weather data, a specified vegetation type, and a specified disturbance regime (a 'spin-up' run). The endpoint of the spin-up run is assumed to represent the state variables averaged over a region large enough to encompass stands in all stages of development: from stands regenerating after a recent disturbance to very old stands. The steady state is only attained as a temporal average, with significant interannual variability remaining due to variation in the surface weather records. In most cases several thousand model years elapse before reaching this steady state, the length of time controlled largely by rates of nutrient input and loss, which together with climate and vegetation physiology control the accumulation and loss of slowly responding soil organic matter pools.

The spin-up run is usually driven by repeated use of a shorter weather record. Longer records are desirable, since they capture greater ranges of interannual variability, and so better represent long-term site climate. For the Y *and* O sites, the onsite measurement records are rather short (< 5 years), with significant data gaps. We therefore made use of a new data base of gridded daily surface weather variables spanning 18 years (1980–97), interpolated from daily observations, and corrected for variations in elevation, slope, aspect and local horizontal

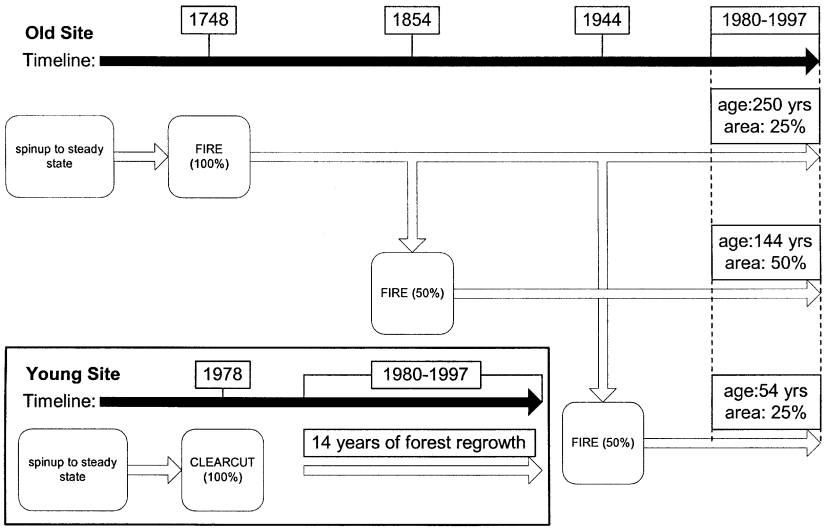

Fig. 3 Schematic of Biome-BGC simulation sequence representing the known details of disturbance history at the Y *and* O sites. Disturbance event timing is shown above the black timeline, with the resulting ensemble of model runs shown as unfilled arrows. The final analysis period is shown between dashed lines for the O site, with current ages and proportional areas shown for each of the three ensemble components assumed to make up the current stand. Regeneration dynamics following clearcut at the Y site are represented with a single age class (inset).

climate gradients (Thornton *et al*. 1997; Thornton & Running 1999; Thornton *et al*. 2001). The data base is gridded at a 1-km resolution, and the cells closest to the Y *and* O sites were extracted and used for all model runs described here. Methods and detailed analyses of estimation error are described elsewhere, but we note here that errors in daily temperature are on the order of 1 °C, daily radiation on the order of 2.5 MJ m^{-2} day^{-1}, and precipitation (in this region) on the order of 10–15% $year^{-1}$.

Most of the parameters required as input to the vegetation ecophysiology component of Biome-BGC were measured at the two sites, or could be derived from measurements at the sites. In some cases, parameters that were not measured onsite were estimated from other published observations of ponderosa pine systems. Measurements of $A–C_i$ curves from both sites, with coincident observations of specific leaf area and leaf C : N, were used to estimate values for the fraction of leaf N in Rubisco. We made site-specific measurements of other driving variables, such as litter, fine root and soil lignin and carbon content, tissue nitrogen content, and maximum and minimum stomatal conductance.

A sequence of simulations was designed to represent the recent history of disturbance and/or management at each site. Following the spin-up runs, a sequence of disturbance and post-disturbance recovery simulations was performed to simulate the effects of either fire (O site) or clearcutting (Y site) on the carbon and nitrogen state variables (Fig. 3). At the O site, the disturbance history was interpreted as a stand-replacing fire that initiated the current 250-year-old age class, a burn approximately 100 years later that affected 50% of the regenerating stand, initiating the middle age class, and another fire approximately 100 years later that affected 50% of the remaining old age class, initiating the current 50-year-old age class. The exact timing of the disturbances was shifted to align with the repeat cycle of the 18-year surface weather record, to allow consistent use of the final 18 years of this ensemble of runs to represent the recent past (Fig. 3). At the Y site, a clearcut disturbance was implemented at the spin-up endpoint, using observations from the site to parameterize the amounts of woody material removed and left onsite. As the dominant age class was only 15-year-old, yet the clearcut took place 21 years ago, the simulation included 7 years of bare site conditions, during which woody detritus and soil organic matter processes continued in the absence of regenerating vegetation (Fig. 3, inset).

The model produces daily estimates for about 500 different water, carbon and nitrogen storage and flux components. We summarized the results to correspond as closely as possible with the wide range of measurements taken at the sites, which focused primarily on the storage and flux components of the site carbon budgets. Comparisons for each relevant component were made on both an absolute and a relative basis (percentage difference between model and observed). Seasonal cycles of the major carbon budget components were summarized for both sites.

For the O site, eddy covariance observations were available for the final 2 years of the 18-year surface weather record (1996 and 1997). We compared model estimates and eddy covariance observations of daily total evapotranspiration (ET), daily gross ecosystem production (GEP) and daily net ecosystem exchange (NEE) for these 2 years. We used only covariance measurements with less than 75% of the flux data missing, following screening. We removed flux data from the analysis when rain had fallen between 9 pm the previous day and 9 pm of the day of interest. We combined the results of the

Table 4 Leaf area index (m^2 of half-surface leaf area per m^2 ground area), sapwood area, ratios of leaf area to sapwood area and volume for 16 ponderosa pine sites east of the Cascade Mountains, Oregon. Standard error in parentheses.

Plot	Size class (d.b.h. in cm)	Sapwood area ($cm^2\ m^{-2}$)	Overstorey LAI ($m^2\ m^{-2}$)	Sapwood area : LAI	Sapwood volume : LAI
1	0–30	24.80	2.0 (0.03)	0.07938	3391
1	30+	17.13		0.05207	19874
2		37.47	0.9 (0.01)	0.06492	44791
3		19.75	2.4 (0.04)	0.07065	22771
4	0–30	19.25	1.4 (0.05)	0.10226	364
4	30+	28.20		0.07177	31380
5		31.96	2.0 (0.02)	0.08681	11739
6		25.81	2.0 (0.03)	0.09824	10079
7		9.25	2.8 (0.03)	0.05285	10702
9		13.33	0.5 (0.01)	0.05993	13849
10		23.57	0.8 (0.03)	0.08512	16506
11		8.96	2.0 (0.01)	0.16765	9065
15		23.49	1.5 (0.04)	0.06134	11061
16		20.67	1.4 (0.03)	0.12544	9389
17		26.79	2.6 (0.14)	0.02673	16384
18		10.79	0.7 (0.02)	0.08956	9018
19		5.80	1.0 (0.02)	0.10494	73834
20		24.80	0.6 (0.02)	0.07938	11178

budget-based comparisons with the eddy covariance-based comparisons to draw some general conclusions about the model performance and the likely implications for the controls on net carbon exchange at the two sites.

The model simulations described above include the effects of increasing atmospheric concentration of CO_2, as described by the IS92a data set (Schimel *et al*. 1994). We also conducted a second parallel sequence of model simulations using an atmospheric CO_2 concentration held constant at pre-industrial levels. Comparing these two sets of simulations allowed us to estimate the relative importance of changing atmospheric chemistry on NEE at these sites, including the possible interactions of changes in atmospheric chemistry and changes in ecosystem state following disturbance.

Finally, we examined the differences in observed allocation patterns between the two sites and conducted a series of model runs to represent the dominant changes in allocation related to developmental stage. These results were used to draw some conclusions about the likely future course of carbon source–sink dynamics at the sites.

The entire Biome-BGC model, including a user's guide, example input and output files, and pre-compiled executables for PC and Unix platforms, is available via the 'Models to Download' section at the web site http://www.forestry.umt.edu/ntsg. Input files used to produce the results in this manuscript are available upon request.

Results and discussion

Environment

Monthly total solar radiation, mean vapour pressure deficit (*D*) and summed precipitation were similar at both sites, although precipitation was slightly greater in summer and annually at the Y site (552 mm Y site vs. 524 mm O site; Fig. 2). Thus, all else being equal, we would expect that summer water stress would be about the same at the two sites, or slightly less at the Y site.

The soil environment was different due to a more open canopy and exposed soils at the Y site, resulting in greater seasonal and diurnal amplitude in soil temperature. Soil temperature often reached 30–40 °C at 2 cm depth in summer at the Y site. Soil moisture at 10 and 30 cm depth declined at comparable rates at both sites to similar seasonal minima of 6% and 8% volumetric water content, respectively.

Leaf area index

The 15-year-old pine forest has not yet reached maximum canopy cover following logging, and based on data from the 16 plots, it isn't likely to reach this point for another 10–20 years. LAI(Y) (1.0 m^2 half-leaf surface area (hsa) per m^2 of ground area; 0.4 of this value was understorey shrubs) was half of LAI(O) (2.1, where 0.12 of this value was understorey shrubs). LAI of trees on the 16 plots of various ages (including Y *and* O sites) ranged

Table 5 Carbon storage for 15-year-old (Y) and 50/250-year-old (O) ponderosa pine sites, in g C m^{-2}

	O site	Y site
Above-ground vegetation carbon		
Wood (bark, branch,stem)	10521(1565)	519 (97)
Foliage (trees)	270	60
Above-ground tree mass	10791	579
Understorey wood mass	0	265 (13)
Understorey foliage mass	16	57
Above-ground understorey mass	16	322
Total above-ground living mass	10808	901
Below-ground vegetation carbon		
Coarse root mass (trees)	1500	63
Fine root mass (total)	423 (95)	500 (75)
Total below-ground living mass	1923	563
Other		
Coarse woody detritus (> 10 cm diameter)	1204 (402)	2092 (215)
Fine woody detritus (1–10 cm diameter)	121 (42)	443 (157)
Litter mass (foliage, litter <1 cm diameter)	1233	708
Fine root detritus[a]	317	335
Coarse root detritus[b]	45	587
Soil C (to 1-m depth)	5330	4310
Total ecosystem C storage	20981	9939
Biomass/Total C storage (%)	61	15

[a]Turnover rates of fine roots from minirhizotron data is 77% and 60% at O *and* Y sites, respectively (C. Andersen, personal communication)

[b]Assuming 3% mortality rate at O site (S. Green, personal communication), and assuming coarse root mass at Y site from previous forest is the same as that of the 250-year-old plot (plot 2) minus the amount that has decomposed over the 21 years since the site was clearcut.

from 1.0 to 2.6 (mean 1.6, SE 0.18; Table 4), and total LAI including understorey averaged 2.0 m^2 hsa m^{-2}. Earlier modelling activities suggest that LAI of ponderosa pine in this region is limited to <3 over the long-term by the site water balance (soil water storage and growing season precipitation minus evapotranspiration) and nutrient deficiencies (Runyon *et al*. 1994; Waring & Running 1998; Law *et al*. 2000a; Law *et al*. 2000b). At the site level, the leaf area : sapwood area ratio of trees was greater for the Y vs. O pine site (0.104 vs. 0. 077). Gower *et al*. (1997) also found that this ratio was significantly greater for young vs. old jack pine. On an individual tree basis, studies suggest that more sapwood is required to support a given amount of leaf area in larger trees, possibly because of hydraulic limitations in large trees (Ryan *et al*. 2000).

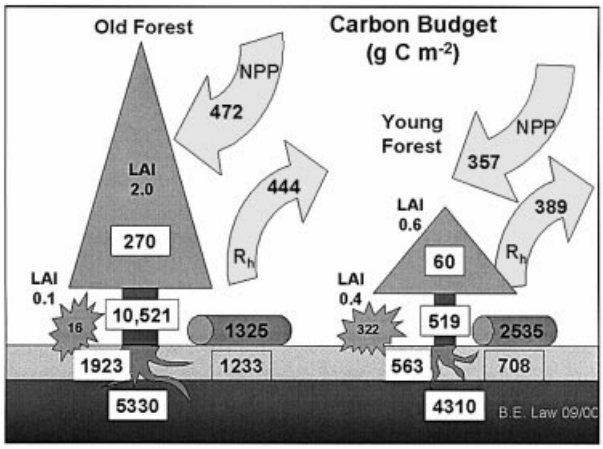

Fig. 4 The annual carbon budgets of the 14-year-old and 45/250-year-old ponderosa pine forests.

Carbon storage

The distribution of carbon differed substantially between the two sites (Table 5; Fig. 4). Soil carbon was consistently lower at all soil depths at the Y site compared to that of the O site (Table 2), and assuming that pre-disturbance conditions were similar between sites, it is in agreement with studies showing decreased soil carbon following disturbance (Schlesinger 1985; Post & Kwon 2000). Total ecosystem carbon content (vegetation, detritus and soil) of the O forest was about twice that of the Y site (21 vs. 10 kg C m^{-2} ground). The most notable difference is that significantly more of the total ecosystem carbon is stored in living vegetation at the O (61%) compared with Y site (15%), while soil carbon is 26% and 43% of the total, respectively.

Fine and coarse woody detritus, including standing dead trees, accounts for a much larger portion of the total ecosystem carbon content at the Y site (25%) compared with the O site (7%), and woody detritus at the Y site was twice that of the O site (Table 5). This is contrary to common expectations that old forests have a large amount of woody detritus compared with young forests. Management practices, however, must be taken into account; in regenerating forests, large amounts of detritus remain onsite after logging of the previous forest (Harmon *et al*. 1990), and old forests often consist of mixed ages and patches of young trees growing in gaps because of fire suppression and stand dynamics. Standing dead trees accounted for about half of the coarse woody detritus at the O site. Litter mass at the O site was almost twice that of the Y site (1233 vs. 708 g C m^{-2}), because more time has passed since disturbance, allowing time for litter accumulation. Monleon *et al*. (1997) demonstrated the importance of

Table 6 Carbon fluxes (respiration and net primary productivity) for the 14-year-old (Y) and 45/250-year-old sites (O). Standard errors are in parentheses.

Component fluxes (g C m^{-2} $year^{-1}$)	O site	Y site
Above-ground		
(1) Respiration of tree foliage	131 (13)	60 (10)
(2) Respiration of understorey foliage	5	64 (11)
(3) Respiration of tree wood	63	3
(4) Leaf and wood detritus production (< 1 cm diameter)	132 (19)	50 (8)
(5) Tree wood production	81 (18)	33 (2)
(6) Tree foliage production	76	23
(7) Total tree ANPP	157	56
(8) Understorey ANPP	16	21
(9) Total ANPP	173	76
(10) Transport to roots (15 – 4 + 12)	671	614
Below-ground		
(11) Respiration of live roots	372	333
(12) Coarse root production (25% of wood production)	23	10
(13) Fine root production (10–11–12)	276	271
(14) Total root production (12 + 13)	299	281
(15) Total soil surface CO_2 efflux	780 (143)	654 (87)
Detritus		
(16) Coarse woody detritus decomposition	33	56
(17) Fine woody detritus decomposition	3	12
Above- and below-ground sums		
(18) Heterotrophic respiration (15 – 11 + 16 + 17)	444	389
(19) Autotrophic respiration (1 + 2 + 3 + 11)	571	445
(20) Ecosystem respiration (18 + 19)	1014	835
(21) NPP (9 + 14)	472	357
(24) NEP (21 – 18)	28	–32
(25) NEP (Monte Carlo)	167 (SD 69)	–68 (SD 21)
(25) NPP/GEP (21/(19 + 21))	0.45	0.45
(26) MRT in years (litter mass/litterfall)	9	14

litter accumulation, and thus nutrient availability, to productivity of old pine forests.

Productivity

Above-ground net primary productivity (ANPP), including shrubs, was greater at the O site (173 vs. 76 g C m^{-2} $year^{-1}$), and shrubs accounted for 27% of ANPP at the Y site, whereas only 10% of ANPP at the O forest was attributed to shrubs (Table 6). At the O site, within the footprint of the flux tower, ANPP ranged from 100 in a pure stand of 250-year-old trees, to 137 in a mixed age stand and 236 g C m^{-2} $year^{-1}$ in a dense 50-year-old stand. Across the 15-km swath of pines, ANPP ranged from 76 g C m^{-2} $year^{-1}$ at the Y site to high values of 220–236 g C m^{-2} $year^{-1}$ for stands aged 46–60 years old (overall mean 158 ± 14 g C m^{-2} $year^{-1}$; Table 7; Fig. 5). Thus, the lowest ANPP values were for the youngest and oldest stands, but there was a large range of ANPP for mature stands, probably due to differences in stand management (e.g. thinning), water availability and nutrients (Grier *et al*. 1981; Gower *et al*. 1994).

There was no significant difference in annual soil flux (780 ± 143 g C m^{-2} $year^{-1}$ O site vs. 654 ± 87 g C m^{-2} $year^{-1}$; Table 6). Standard errors of the measurements averaged 9.1% at the O site, and 6.7% at the Y site. Root respiration accounted for 49% ± 12 and 43% ± 8 of total soil surface CO_2 efflux in May at the Y *and* O sites, 53% ± 8 and 53% ± 11 at the Y *and* O sites in July, and 53% ± 8 and 42% ± 8 at the Y *and* O sites in October. Annual litterfall was greater at the O site (132 vs. 50 g C m^{-2} $year^{-1}$; $P < 0.01$; Table 6), because of the presence of twice the leaf area of the Y forest. Below-ground net primary productivity (BNPP), calculated from the difference between below-ground C allocation and root respiration, was 299 and 281 g C m^{-2} $year^{-1}$ at the O *and* Y sites, and NPP_{fr} was 60% and 76% of total NPP (Table 6). Comeau & Kimmins (1989) showed that NPP_{fr} accounted for *c.* 55% of total NPP in xeric lodgepole pine stands, a greater proportion than observed at more mesic sites. On average, evergreen coniferous forests allocate *c.* 40% of carbon to root production (Gower *et al*. 1997; Vogt *et al*. 1986). Total NPP was higher at the O site (472 vs. 357 g C m^{-2} $year^{-1}$),

Table 7 Above-ground biomass and net primary production (ANPP) at 16 ponderosa pine sites. Standard errors in parentheses.

	Biomass (g C m^{-2})				ANPP (g C m^{-2})	
Plot	Mean age	Foliage	Wood	Total	Foliage	Wood	Total
1	50, > 250	259	8603 (938)	8862	73	64 (4)	137
2	> 200	133	11136 (1174)	11269	37	63 (4)	100
3	56 (9)	363	13542 (3196)	13905	102	134 (18)	236
4	11 (1), 160	208	14574 (4487)	14782	58	163 (44)	221
5	77 (4)	294	5484 (1423)	5778	82	122 (15)	204
6	77 (6)	302	4888 (801)	5190	85	123 (11)	208
7	97 (15)	163	7014 (1538)	7177	94	133 (20)	227
9	61 (5)	73	1895 (268)	1968	20	87 (8)	107
10	30 (5)	119	1656 (181)	1775	34	93 (7)	127
11	46 (8)	299	5219 (325)	5518	84	139 (7)	223
15	57 (8), 129 (30)	224	4050 (780)	4274	63	48 (7)	111
16	67 (9)	215	5838 (1012)	6053	60	106 (11)	166
17	57 (3)	156	5039 (1950)	5195	91	127 (25)	218
18	175 (40)	60	12533 (2944)	12593	27	55 (11)	82
19	61 (6)	144	2497 (496)	2641	40	74 (9)	114
20	14 (1)	112	615 (57)	728	41	35 (NA)	76

and the ratio NPP/GEP was the same (0.45). Previously, we used eddy flux and chamber data for a full year at the O site to determine GEP, and this resulted in a NPP/GEP ratio of 0.47.

Ecosystem respiration

Fresh tree foliage litter decomposed more rapidly at the O site (81.6% ± 2.6 vs. 86.1% ± 0.6 mass remaining at the Y site), yet the lignin fraction was higher than that of the Y site (41% vs. 35%), so the differences appear to be minor. Fine root decomposition rates were similar (87.8% ± 3.9 and 87% ± 0.9 mass remaining after 1 year at the O *and* Y sites).

Measurements of woody detritus respiration in July showed that at *c.* 25 °C, respiration averaged 1.2 μmol m^{-2} wood s^{-1} for several hours following rain, but decreased to zero as the wood dried in the next couple of days. Thus, respiration from woody detritus is strongly controlled by temperature and moisture conditions, and probably occurs in very short-term pulses during the year (e.g. primarily in spring and fall when temperatures are relatively warm and there is moisture available). The CO_2 lost to the atmosphere annually from decomposition of coarse and fine woody detritus was 36 g C m^{-2} at the O site, and 68 g C m^{-2} at the Y site (Table 6). Previous studies have shown that decomposition rates of standing dead pines are much slower than coarse woody detritus on the ground (e.g. 0.3% vs. 2.5%; Yatskov 2000) due to less contact with decomposers. Thus, we probably overestimated decomposition at the O site by *c.* 10 g C m^{-2} $year^{-1}$ because we used the log decomposition rate for standing dead trees.

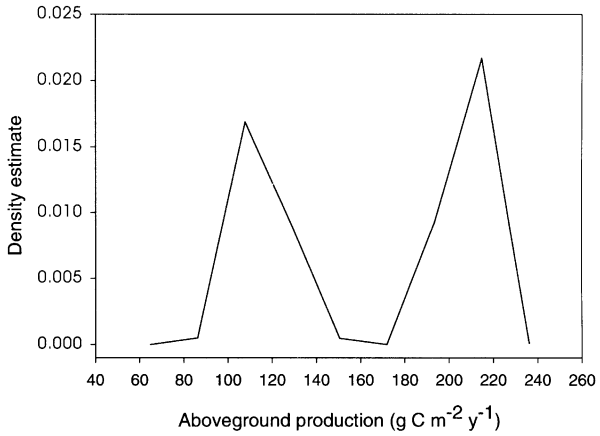

Fig. 5 The probability density function of above-ground net primary productivity (ANPP) at 16 ponderosa pine sites.

Ecosystem respiration (R_e) from the soil surface, foliage, sapwood and detritus was higher at the O site (1014 vs. 835 g C m^{-2} $year^{-1}$), and soil fluxes accounted for 77% of R_e at both sites (Fig. 6). Assuming a decomposition rate of 2.7% per year at both sites, coarse and fine woody detritus decomposition was 36 and 68 g C m^{-2} $year^{-1}$ at the O *and* Y sites, and accounted for a small portion of heterotrophic respiration (8% and 18%, respectively). Respiration from decomposing coarse root detritus was about 16 g C m^{-2} $year^{-1}$, assuming that the forest logged 20 years ago was similar to plot 2, and

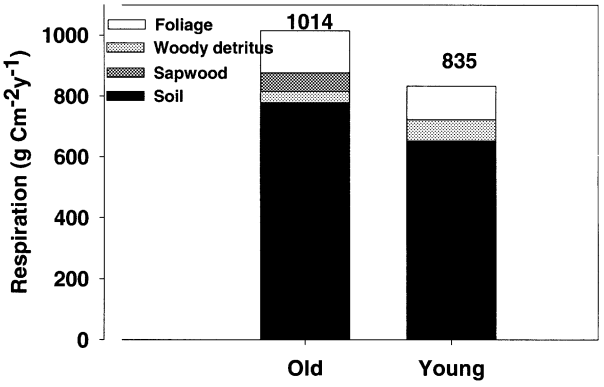

Fig. 6 Ecosystem respiration in 1999, estimated from chamber data and site-specific temperature response equations, was greater at the O site. Soil surface CO_2 effluxes accounted for *c.* 77% of the total at both sites.

decomposition rates were similar to that of coarse woody detritus (k = –0.027; Table 6).

Net ecosystem production

Net ecosystem production (–NEE = NEP = NPP – R_h) estimated from field measurements, was 28 and –32 g C m^{-2} $year^{-1}$ at the O *and* Y sites (Table 6). We used alternative methods for estimating components of NEP in a Monte Carlo approach to compute a mean value and error in the estimate (Harmon *et al*. 2001). We assumed that differences in measurement methods lead to the greatest differences in estimates of NEP. We estimated fine root production from turnover rates and fine root biomass in October at each site (NPP_{fr}(O) = 618, NPP_{fr}(Y) = 238), foliage production from foliage litterfall (NPP_{fol}(O) = 87, NPP_{fol}(Y) = 40), and annual soil fluxes from almost a year of automated soil chamber data (554 g C m^{-2} $year^{-1}$ at Y site, no difference at O site). We used these estimates and values for the same variables shown in Table 6 in the Monte Carlo model. The Monte Carlo estimate of mean NEP(O) was 167 g C m^{-2} $year^{-1}$ (SD 69; 95% CI is 31–305 g C m^{-2} $year^{-1}$), and NEP(Y) was –68 g C m^{-2} $year^{-1}$ (SD 21; 95% CI is –80 to 4 g C m^{-2} $year^{-1}$). Thus, the 15-year-old forest appears to be a source of CO_2 to the atmosphere because heterotrophic respiration, primarily from soils, is large compared with carbon uptake of the regrowth. Schulze *et al*. (1999) found similar results in Eurosiberian boreal forests, where regrowth forests remain net sources of CO_2 to the atmosphere for at least 14 years after logging, and they are weaker sinks for atmospheric CO_2 than are nearby old-growth forests.

Because eddy flux data were missing over long periods, we were not confident in annual estimates from these measurements. However, in 1996 (a wet year) and 1997 (a very dry year), eddy flux estimates of NEE at the O site were –324 ± 168 and –266 ± 177 g C m^{-2} $year^{-1}$; these values are within the limits of our biological estimates. Errors in the approaches to estimating NEE (eddy covariance approach) and NEP (biological approach) are large, but combining biological and eddy flux data is useful for model testing.

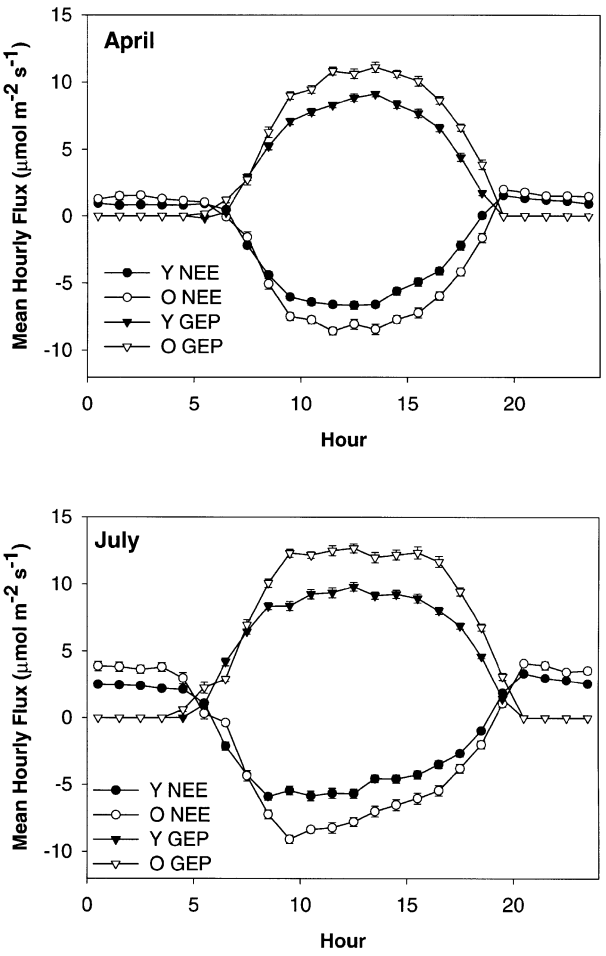

Fig. 7 Average diurnal gross and net CO_2 fluxes were greater at the O site than the Y site in (a) April and in (b) July when drought stress was evident. Gross ecosystem production (GEP) was calculated from chamber estimates of daytime ecosystem respiration and eddy covariance estimates of daytime net ecosystem exchange of CO_2 (NEE).

Seasonal CO_2 and water vapour exchange

Eddy covariance data were averaged in April and July to show diurnal differences in carbon exchange (Fig. 7). Daytime net uptake of CO_2 and GEP were greater at the O site than the Y site through most of the year, particularly in August and September when drought

stress in the young trees was most severe. In April, the daily GEP(O) averaged 4.4 and GEP(Y) 3.4 g C m^{-2} day^{-1}, and mean 24 h NEE(O) was –1.3 and NEE(Y) was –1.0 μmol m^{-2} s^{-1}. Some snow was still on the ground at the Y site in April, and air temperatures from January through April were consistently 1 °C cooler than at the O site. GEP and net uptake of CO_2 were also greater at the O site than the Y site in July (mean daily GEP(O) 6.0 and GEP(Y) 4.5 g C m^{-2} d^{-1}; mean 24 h NEE(O) –0.9 and NEE(Y) –0.6 μmol m^{-2} s^{-1}). The proportion increase in GEP from April to July was about the same (36% at the O site, 32% at the Y site), and GEP was *c.* 25% greater at the O site than the Y site. Although net CO_2 uptake decreased at both sites in July compared with April, it was *c.* 25% greater at the O site, suggesting that gross photosynthesis was more responsible than respiration for site differences in NEE.

Water vapour exchange (λE), including evaporation from all surfaces, was lower at the Y site than that of the O site in April and July. Daily average tree transpiration from May to June was similar at both sites (0.81 mm day^{-1} O site, 0.82 mm day^{-1} Y site), but lower at the Y site through July and August (1.06 mm day^{-1} O site, 0.69 mm day^{-1} Y site). This pattern was probably a consequence of limited water availability due to shallow rooting of the trees at the Y site (Williams *et al*. 2000; Irvine & Law 2001). The maximum carboxylation rate, V_{cmax} normalized to 25 °C, was similar for trees in June (25 ± 2 and 25 ± 3 μmol m^{-2} s^{-1} for the Y and O site, respectively), but it was significantly greater at the Y site in August (39 ± 2 vs. 32 ± 2 μmol m^{-2} s^{-1}). Values were slightly higher for shrubs than trees at the Y site. The higher V_{cmax} per unit leaf area at the Y site than the O site probably offset lower carbon assimilation as a consequence of lower LAI and reduced canopy conductance at the Y site, so that between-site differences observed in GEP were not as large as we might expect. Interestingly, when rainfall was 20% lower in 2000, V_{cmax} was similar for trees in June at the Y and O site, but it was significantly lower at the Y site in August.

Biome-BGC Modelling

Comparisons of observations and model simulations

Comparisons between Biome-BGC estimates and measured components of the C budget are summarized in Table 8, where storage and flux components are separated for the two sites. Estimation biases, expressed as a percentage difference between model and observed, are typically much lower for the flux components than for the storage terms. This is the expected result as the model storage terms tend to accumulate the effects of small estimation biases in model fluxes over multiple years.

Modelled leaf area index is slightly different than measured using optical methods (2.6 vs. 2.1 at the O site, 0.7 vs. 1.0 at the Y site). Using observations of foliage NPP, leaf lifespan and specific leaf area, alternative values for observed LAI at the O *and* Y sites are 2.7 and 1.1; which is a much better agreement at the O site, and slightly worse model underestimate at the Y site, in comparison to the optical LAI results.

Among the storage terms, some of the largest errors are in the estimation of soil carbon, litter carbon and woody detritus carbon, with the model overestimating soil organic matter and underestimating the litter and detritus pools. Some bias following this pattern is expected as a result of different definitions of these pools in the model and in the data collection. In the field, for example, litter carbon includes fresh litter as well as some material that has already begun to decay, while the model litter pool includes only the part of the litter that has not been subjected to microbial action. In addition, the field measurements for soil organic matter were made to 1-m depth, while the model accounts for soil organic matter in the entire soil column.

These factors are not likely to explain the entire difference between total litter and soil carbon, suggesting that the model base rate for decomposition of the more recalcitrant soil organic matter pools may be too slow, or that the temperature and moisture controls on this base rate may be inaccurate. These problems do not appear to have a strong effect on annual total heterotrophic respiration rates, which are reasonably close to the observed values at both sites.

Another obvious problem for the storage terms is a large overestimation of total fine root carbon at the O site. The longevity of fine roots is assumed in the model to be the same as for leaves. This assumption appears to be faulty at the O site, and perhaps less so at the Y site, because the model estimates for annual production of fine roots are about 20% lower than observed at both sites. These results suggest that the fine root longevity for the O site should be roughly half the leaf longevity (or about 2 years), with somewhat higher values at the Y site.

A third apparent problem for the storage comparison is a large underestimate of above-ground vegetation carbon (presumably mostly woody biomass) at the Y site. As total NPP is also moderately underestimated at this site, it is possible that this difference reflects the accumulated error. However, the difference in NPP appears to be mostly the result of underestimated fine root production, with excellent agreement between modelled and observed wood NPP. It is possible that the presence of a small number of older trees at the Y site has a strong influence on the observed woody carbon

storage, a factor not represented in the disturbance history for these simulations.

Autotrophic respiration is overestimated at the O site, but is in good agreement at the Y site. Maintenance respiration is assumed to be a function of temperature, biomass, and tissue nitrogen content (Ryan 1991), so much of the O site discrepancy could result from overestimating the standing biomass of fine roots. Offsetting errors in the modelled GEP result in relatively good estimates of total NPP. It should be noted that the 'observed' GEP values are derived largely from empirical models, and so the comparison is of one model against another for this term.

The ratio of model NPP/GEP is lower at both sites than observed, suggesting that the base rate for the maintenance respiration algorithm may be too high, but again it is difficult to draw conclusions given the uncertainty in observed GEP.

Comparison of individual components of NPP shows good agreement between modelled and observed values, except for the underestimation of fine root NPP already noted, which carries over to a smaller percentage underestimate in total below-ground NPP. The model represents both the relative allocation to different components, as well as the absolute NPP components with reasonable accuracy.

Soil carbon flux is slightly overestimated at both sites, while the component coming from heterotrophic respiration is moderately underestimated at the O site. The comparison against monthly root respiration observations supports the conclusion that an overestimate of fine root longevity at the O site leads to an overestimate of standing fine root biomass and an overestimate of fine root maintenance respiration. Agreement with monthly fine root respiration observations is within the measurement error at the Y site. Total ecosystem respiration is overestimated at the O site by an amount that could be explained by an error in fine root maintenance respiration.

The largest percentage differences in the flux term comparison are for NEP. At the O site, the model estimates an average sink of 60 g C m^{-2} $year^{-1}$ over the period 1980–97, with an interannual standard deviation of 24 g C m^{-2} $year^{-1}$. In absolute terms this agrees well with the observed NEP as calculated from the other measured budget components (28 g C m^{-2} $year^{-1}$), but since the net fluxes are close to neutral, the percentage error is large. Comparison of Biome-BGC NEP with the Monte Carlo estimates and eddy flux covariance estimates are increasingly poor, with a model underestimate of more than 240 g C m^{-2} $year^{-1}$ compared to eddy flux data. For this difference to be real, there would need to be a corresponding accumulation of carbon either in the vegetation or in the soil; for example, NPP 53% higher than observed with the same heterotrophic respiration, or NPP as observed but heterotrophic respiration 56% less. No reasonable explanation from the other component comparisons can explain this difference, and it appears from the rest of the budget component measurements that the Monte Carlo estimate is close to a reasonable upper limit for the sink strength at the O site. The model predicts that the Y site is still a net carbon source after 14 years of regrowth, which is in rough agreement with NEP based on budget calculations and on Monte Carlo estimates. Annual totals for the eddy flux method are not yet available for comparison at the Y site.

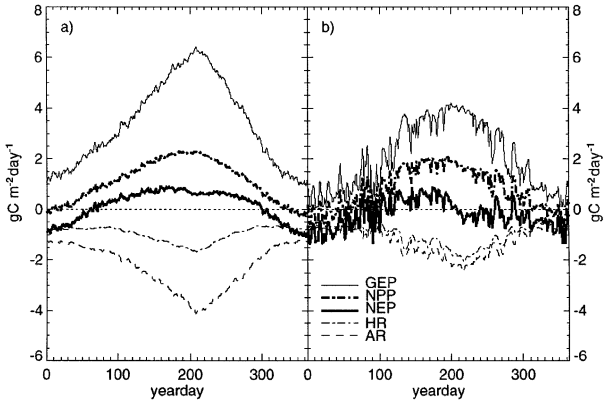

Fig. 8 Seasonal cycle of major carbon budget components; (a) 18-year average (1980–97) for O site and (b) the final year of 14-year post-clearcut simulation at Y site. Dotted line shows the zero reference.

Simulated seasonal and annual fluxes

Figure 8 shows the seasonal cycle of major flux components at both sites, averaged over 14 years at the O site, and taken as the final year in the 14-year regrowth simulation at the Y site. Trajectories for NEP at the two sites are very similar in the winter, spring and early summer, with a consistent net daily source to the atmosphere averaging around 1 g C m^{-2} day^{-1} in mid-winter, crossing to a net sink in April, and rising to a net sink of less than 1 g C m^{-2} day^{-1} by mid-July. The patterns through late summer and into the fall are very different at the two sites. At the O site, higher LAI allows NPP to rise during the peak heterotrophic respiration (R_h) period, maintaining a net sink through the end of October. At the Y site, with similar amounts of soil organic matter, R_h increases through mid-summer but lower LAI in the immature stand keeps NPP flat, and NEP shifts to a source again by late July.

Daily flux data from the eddy covariance systems are available from the O site for 2 years overlapping with the 18-year surface weather record (1996 and 1997). Figure 9 shows the comparison of model and observed daily total

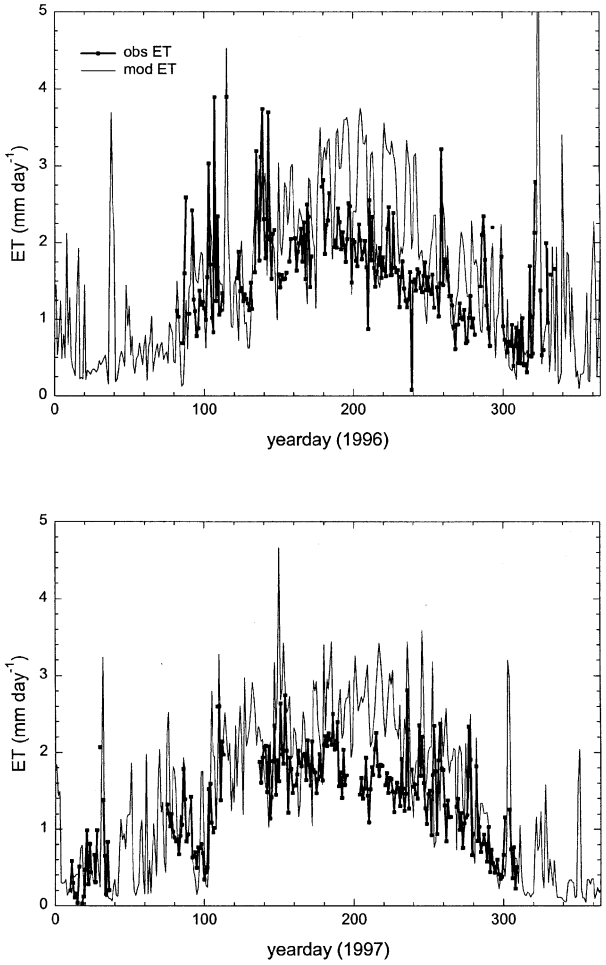

Fig. 9 Daily flux comparison for ET at the O site, (a) 1996 and (b) 1997.

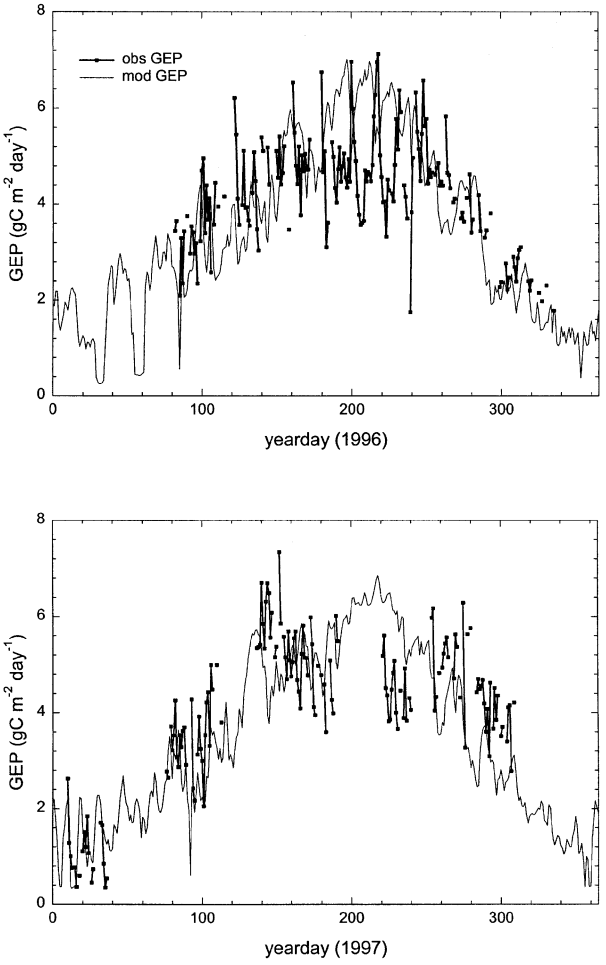

Fig. 10 Daily flux comparison for GEP at the O site, (a)1996 and (b) 1997.

evapotranspiration (ET, includes evaporation from all surfaces) for these 2 years. Observations are not available for every day. The correspondence is very good through the end of June, including both the seasonal trends and the daily variation. From July through September, the model consistently overestimates daily ET by 1–1.5 mm day^{-1}, after which the correspondence is good again. Almost exactly the same pattern of bias through the late summer is observed in both years. This result suggests that the site experiences some degree of water stress that the model is not reproducing.

A very similar story emerges for the daily comparison of model and observed GEP (Fig. 10). The agreement is good in the winter and spring, with a pronounced overestimate of GEP during July and August. There is an interesting pattern in the mid-summer period for the 1996 comparison (Fig. 10a). There are at least three to four cycles of high model GEP and low observed GEP, with short periods in between when the model GEP drops exactly as the observed GEP rises. Examination of the surface weather records shows that each of these episodes of rapidly falling model GEP at the time of rapidly rising observed GEP is characterized by a pronounced drop in air temperature and a decrease in daily total radiation: a cloudy cold front. The model predicts that the cold temperature and lower radiation is reducing the canopy photosynthetic potential, while the observations suggest the opposite. Anthoni *et al*. (1999) suggest that this peak in eddy flux NEP is the result of increasing GEP due to reduced vapour pressure deficit (VPD) and related increases in stomatal conductance. The pattern of model over-predictions of mid-summer ET and GEP, together with the inverse relationship to eddy flux NEP during cold front passage, suggests that the model sensitivity to VPD is too weak for this site.

Comparison of model and observed daily NEP in 1996 (Fig. 11a) shows that each of these cold episodes corresponds to a dramatic rise in observed NEP. This response

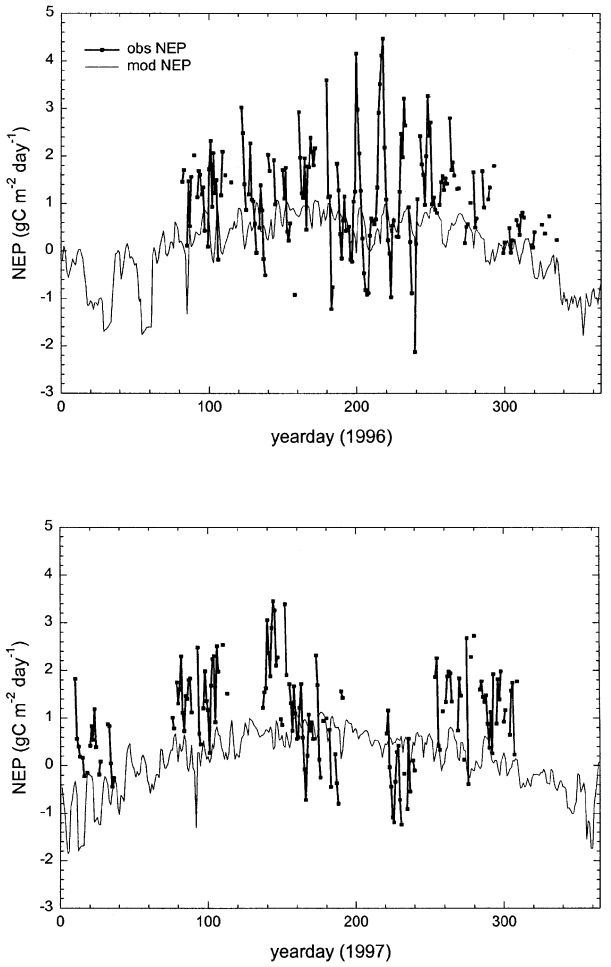

Fig. 11 Daily flux comparison for NEP at the O site, (a) 1996 and (b) 1997.

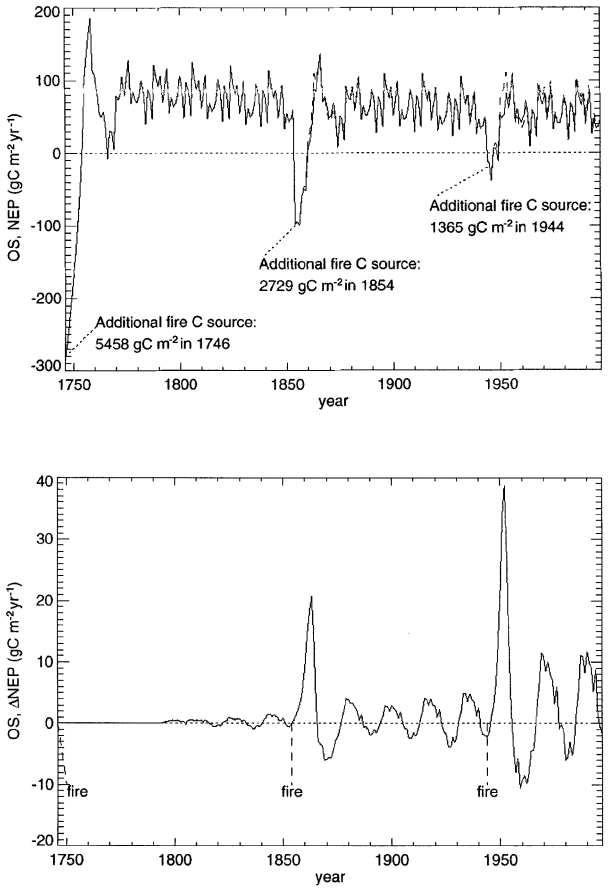

Fig. 12 Simulated trajectory of NEP at the O site showing: (a) the influence of disturbance history, interannual variation in climate, and changing atmospheric concentration of CO_2; solid line is with constant CO_2 at preindustrial level, dashed line is observed historical CO_2; and (b) isolated influence of increasing CO_2 on O site NEP (difference between increasing CO_2 run and constant CO_2 run).

could be due to a large drop in autotrophic and/or heterotrophic respiration, and a large increase in canopy photosynthetic potential because VPD is not as constraining. A general conclusion from the NEP comparisons for both 1996 and 1997 is that the observed daily variation in NEP is much greater than that predicted by the model. There is in general much less consistency between the years in the NEP comparison than for either ET or GEP. Observed NEP in winter, spring and autumn is uniformly higher than predicted by the model, which may be due to differences in respiration estimates because the GEP estimates were similar during this period.

Influence of climate variability, disturbance and increasing CO_2

Annual NEP from the 250-year ensemble simulation for the O site shows the combined influence of disturbance history, interannual climate variability and changing atmospheric CO_2 concentration (Fig. 12a). Interannual variability in NPP and in heterotrophic respiration is of similar magnitude, and these variations combined with differences in climate response between the two are responsible for the patterns of interannual variability in NEE.

The relative influence of the three disturbance events in this ensemble is related to the fractional area assumed affected by each event (Fig. 3). Ignoring the direct source of CO_2 to the atmosphere during combustion, the effect of post-fire ecosystem dynamics on the variability in NEP for this site is 2–4 times larger than the effect of interannual climate variation. When the direct combustion sources are considered, the 1-year disturbance effect is in the order of 10–20 times as large as the effect due to interannual climate variation.

The influence of increasing atmospheric concentration of CO_2 on simulated NEP over the 250-year site history was estimated by subtracting a constant-CO_2 simulation from the IS92a CO_2 simulation (Fig. 12b). Three effects are obvious from this analysis: (i) a gradual trend toward increasing sink strength over the 250-year record; (ii) an amplification of the effect of interannual climate variability as CO_2 concentration increases; and (iii) an interaction with the disturbance process that becomes increasingly important as the CO_2 concentration increases. The cyclic variation in Fig. 12(b) is mostly the result of repeated use of the same 18-year surface meteorological record. Note that although the fractional area affected by the first, second, and third disturbances are 100%, 50% and 25%, respectively, the interaction effect between disturbance and increasing CO_2 concentration shows the largest effect for the smallest disturbance.

Careful analysis of model behaviour during the regeneration phase following disturbance shows that the CO_2-disturbance interaction effect is caused by changes in the system nitrogen (N) status following disturbance. With a reduced vegetation demand for mineral N immediately following disturbance, and with the microbial N immobilization demand reduced due to the combustion of litter with a higher C : N than the soil organic matter, the availability of N mineralized from decaying soil organic matter is increased. In the early stages of canopy regeneration, total plant N-demand is still relatively low, and the combination of increased carboxylation potential in the presence of higher CO_2 concentrations with increased availability of mineral N results in increased plant growth, compared with the constant-CO_2 case. Rapid growth and canopy expansion during this early regeneration period causes increased plant N-demand, until the combined demand from plant uptake and microbial immobilization cause a new state of mineral N limitation to growth. During this period the effect of higher CO_2 concentration is reduced because the N supply to meet the stoichiometric needs of new plant growth is limiting.

The relative carbon balance effects of disturbance, interannual climate variability and increasing CO_2 concentration can be easily assessed by looking at the total ecosystem carbon content over time (Fig. 13a). It is obvious from this pattern that disturbance history establishes the most important long-term patterns in total carbon loss and gain. This analysis makes it clear that, at least with pre-industrial levels of atmospheric CO_2, nearly 100 years of stand growth are required to return the system to a neutral carbon stocking following a stand-replacing fire. This is in contrast to the single-year net carbon balance expressed as NEE, which shows a net annual sink after only 10–20 years. This distinction is

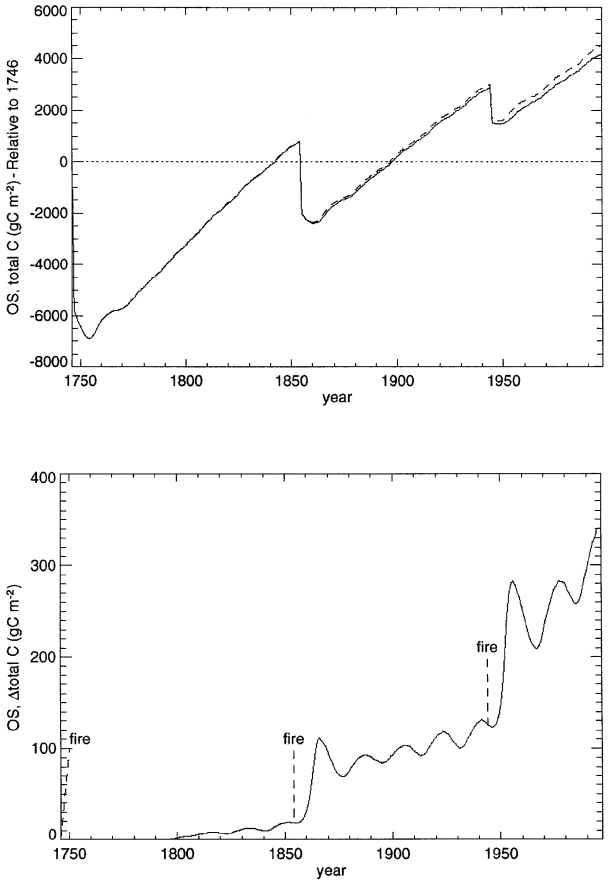

Fig. 13 As Fig. 12, but for the O site total carbon.

particularly important when considering the relevance of forest regeneration to policy discussions of carbon sequestration as an offset to fossil fuel CO_2 emissions (Hoover *et al*. 2000; Murray *et al*. 2000). The effect of increasing CO_2 concentration in this carbon stock recovery process is to increase the recovery rate. This process is most important in the decade following a fire disturbance, and the importance in general increases with increasing CO_2 concentration (Fig. 13b), at least for the current state of disequilibrium between the atmosphere and terrestrial ecosystems (Schimel *et al*. 2000).

The case of regeneration following a clearcut disturbance at the Y site, provides an opportunity to explore the details of the decadal variation in NEP immediately following a stand-replacing disturbance. NPP measurements from the O *and* Y sites show that the proportion of annual growth allocated to new fine roots compared with that allocated to new leaves is higher by a factor of two at the Y site (Table 6). This has important consequences for the rate of increase in NEP during the regeneration process (Fig. 14a). In all cases, model plant N uptake is assumed to be driven by growth demands, and not limited for example by fine root density or fine root

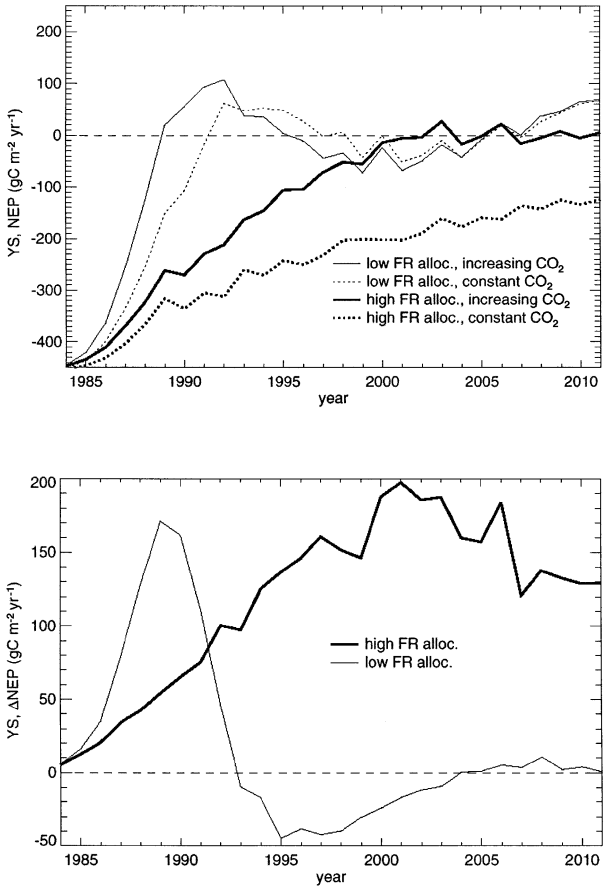

Fig. 14 Simulated trajectory of NEP at Y site showing: (a) influence of disturbance history, interannual climate variability, changing atmospheric concentration of CO_2, and different allocation parameters for the ratio of new fine roots : new leaves; and (b) isolated influence of increasing CO_2 concentration under two different scenarios for fine root allocation.

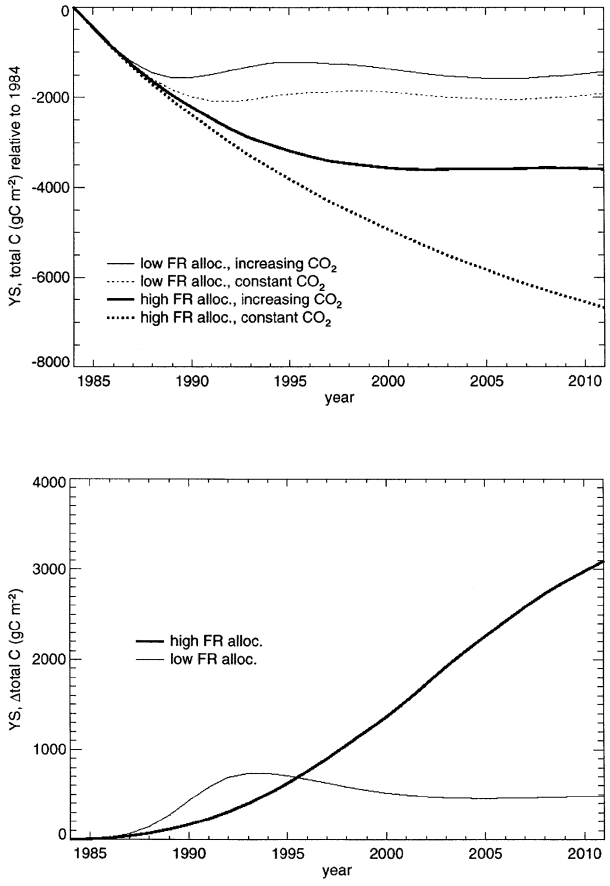

Fig. 15 As Fig. 14, but for Y site total carbon.

surface area (Thornton 1998). Changing below-ground allocation patterns has the effect of changing the carbon resources available for growth of new leaves. In the regenerating canopy, the new leaf deployment rate has a strong effect on the subsequent growth rate, analogous to a compound interest problem. Figure 14(a) shows the post-clearcut regeneration response over 28 years, with the fine root : leaf allocation ratio set to 2.5 (low, characteristic of the mature trees at the O site) and 5.0 (high, characteristic of the young trees at the Y site). The difference between increasing and constant CO_2 concentration is also shown (Fig. 14b).

With high fine root allocation and observed (increasing) CO_2 concentrations, the Y site is predicted to reach a nearly neutral NEP state after about 15 years, or very close to the current stand developmental stage. If fine root allocation remains high, the model predicts that the stand will remain at this neutral NEP state, and never reach the pre-disturbance total carbon storage level (Figs 15a and 15b). Canopy total LAI is also predicted to reach a maximum at 1.0 if the high fine root allocation is maintained indefinitely. The measurements at the two sites suggest, however, that sometime between 15 and 45 years of age the proportional allocation to fine roots decreases.

We hypothesize that the early large investment in fine root growth is required to meet the rapidly increasing demands for water and nutrients from the regenerating canopy, and once the canopy reaches a steady state, and soil space has been occupied, new proportional allocation below-ground can be reduced. As a simple test of the influence of changing fine root allocation on the stand productivity and net carbon exchange, we ran a final simulation with high fine root allocation for 28 years, switching abruptly to low fine root allocation for another 28 years (Fig. 16).

A transient response is observed at the point of changing allocation, which is probably not a realistic response because the real shift is more likely to take place gradually. By the end of the 56-year simulation, there is a

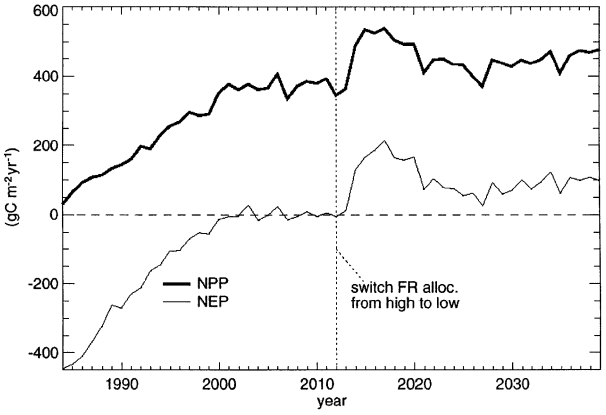

Fig. 16 The influence on NPP and NEP of changing from high fine root allocation to low fine root allocation after 28 years of regeneration following clearcutting at the Y site.

consistent net sink of about 100 g C m^{-2} $year^{-1}$, which is close to what we estimate for the mature stand with a constant low fine root allocation. It is also interesting to note that the values for annual NPP at year 28 (375 g C m^{-2} $year^{-1}$) and at year 56 (475 g C m^{-2} $year^{-1}$) correspond very closely to the observed NPP values for the Y *and* O sites, respectively (Tables 6 and 8). This suggests that the model can produce reasonable NPP estimates at different developmental stages by introducing very limited and well-supported changes in the allocation control. These exercises suggest that the Y site is probably currently very close to the conversion point from a net source to a net sink for carbon, and that future net carbon exchange at the site will depend strongly on the actual time-course of age-dependent changes in the ratio of fine root : leaf allocation.

Finally, it is important to note that the simulations at the Y site have ignored the influence of the shrub component on regeneration dynamics. It is likely that shrubs have important interactions with the tree component of the site vegetation, which could significantly alter the time course of post-clearcut regeneration. The representation of multiple interacting plant functional types is an active area of new development for the Biome-BGC model.

As demonstrated by the use of simulation ensembles to represent the disturbance history at the old site, these modelling results are sensitive to spatial scale. The diversity of disturbance size and intensity increases as larger landscapes are considered, and the influence of any particular disturbance event on the regional exchanges of carbon becomes less important at larger scales (Keane *et al*. 1996). In the case of disturbances that are non-randomly distributed in space and/or time, the contributions from many individual disturbances can have an important effect on regional averages of the net carbon flux. For example, the large wild fires that burned in the western United States in summer of 2000 can be expected to have a more important effect on future regional net carbon fluxes than the same amount of burning spread out over a larger area and multiple years. Another example is the large-scale conversion of land cover related to agriculture and grazing (DeFries *et al*. 1999; Houghton *et al*. 1999).

These results allow us to address only the case of a single climate and a single vegetation type, but the influence of disturbance on net carbon exchange is also likely to vary with mean climate and with vegetation type. The number of sites with such extensive measurements is small, but we hope to take advantage of other such data sets and the modelling methods described here to explore these relationships across gradients in climate and vegetation type.

Conclusions

The greatest difference between sites was that the amount of carbon stored at the O site was more than twice that of the Y site, and 61% of that amount was stored in live biomass compared with 15% at the Y site. A Monte Carlo approach to setting bounds on biological estimates of annual net carbon uptake suggests that the Y site is still a source and the O site is a sink for atmospheric CO_2. Although young forests are expected to be more productive than old-growth forests, in the Pacific North-west, studies suggest that it can take 20–30 years for them to reach maximum canopy cover, and for them to become a net sink for atmospheric CO_2 following stand-replacing disturbance (Cohen *et al*. 1996). Modelling and measurements show that the young regenerating forest has probably not reached maximum canopy cover and leaf area for the site, which limits the potential for gross carbon uptake. Although there was twice the amount of woody detritus at the Y site, differences in decomposition of this material is minimal (32 g C m^{-2} $year^{-1}$), thus woody detritus probably did not contribute much to the differences in NEP between sites. In comparison, NPP(O) was greater than NPP(Y) by >100 g C m^{-2} $year^{-1}$. At both sites, respiration of CO_2 was largely from the soils (77% of total ecosystem respiration), as found in other studies (Goulden *et al*. 1996; Law *et al*. 1999a; Law *et al*. 1999b; D. Ellsworth, personal communication). These results suggest that the net ecosystem production of young stands may be low because heterotrophic respiration, particularly from soils, is higher than the NPP of the regrowth.

The Biome-BGC model suggests that the old forest is a sink for carbon, with interannually varying sink strength of 20–100 g C m^{-2} $year^{-1}$, while the young forest has been a source of carbon since logging. The young forest

Table 8 Comparison of Biome-BGC results with observations from Y and O sites for both carbon storage and carbon flux components. Observed values from Table 5, Table 6 and the text. All storage terms are in units of g C m^{-2} unless otherwise noted. All flux terms are in units of g C m^{-2} $year^{-1}$ unless otherwise noted. For O site, model results from final 18 years (1980–97) are averaged, with interannual standard deviation in parentheses. For Y site, because of rapidly changing conditions over the 14-year simulation, storage and flux results are from the final year only (1997). Standard errors for observed values are shown in parentheses when available. Missing components are shown as '–'. Percentage difference between model and observed values is not calculated for percentage or proportion components.

		Old site			Young site		
	Note	Model	Observed	Difference (%)	Model	Observed	Difference (%)
Carbon storage							
Total ecosystem C		23027 (346)	20981	+10	16117	9939	+62
Total vegetation C		10690 (295)	12731	–16	1010	1464	–31
AG vegetation C		8670 (256)	10808	–20	391	901	–57
BG vegetation C		2020 (41)	1923	+5	618	563	+10
Foliage C		342 (4)	286	+20	117	117	0
LAI (unitless)		2.6 (< 0.1)	2.1	+24	0.74	1.0	–26
Fine root C		854 (11)	423	+102	580	500	+16
Woody detritus C	a	635 (12)	1370	–54	2283	3122	–27
Fine litter C	a	664 (40)	1550	–57	195	708	–72
Soil C	a, b	11037 (4)	5330	+107	12629	4310	+193
Carbon fluxes							
GEP		1240 (47)	1048	+18	750	802	–7
Maintenance resp.		703 (29)	–	–	364	–	–
Growth resp.		124 (5)	–	–	89	–	–
Autotrophic resp.		827 (33)	571	+45	453	445	+2
NPP		413 (15)	472	–13	297	357	–17
NPP/GEP (prop.)		0.33 (0.01)	0.45	–	0.40	0.45	–
AG NPP		178 (7)	173	+3	83	76	+9
BG NPP		235 (9)	299	–21	214	281	–24
Foliage NPP		89 (3)	87	+2	42	44	–5
Foliage NPP (%)		22 (< 1)	18	–	14	12	–
Fine root NPP		227 (8)	276	–18	208	271	–23
Fine root NPP (%)		54 (< 1)	58	–	70	76	–
Wood NPP		98 (4)	109	–10	47	43	+9
Wood NPP (%)		24 (< 1)	23	–	16	12	–
Heterotrophic resp.		353 (12)	444	–21	368	389	–5
Soil C flux		851 (19)	780 (143)	+9	706	654 (87)	+8
May root resp. (%)		58 (1)	43 (8)	–	49	49 (12)	–
July root resp. (%)		58 (1)	53 (11)	–	47	53 (8)	–
Oct root resp. (%)		64 (4)	42 (8)	–	49	53 (8)	–
Total ecosystem resp.		1180 (33)	1014	+16	821	835	–2
	c		28	+114		–32	+119
NEP	d	60 (24)	167 (69)	–64	–70	–68	+3
	e		300 ± 170	–82		–	–

Notes: (a) Observed litter and woody detritus mass includes some partially decomposed material that is included in the soil organic matter pools in Biome-BGC. (b) Observed to a depth of 1 m, while Biome-BGC uses a 2-m soil depth for these simulations. (c, d, e) Three different estimates from observations, using different methods: component budgets, Monte Carlo estimate (SD) and eddy flux covariance (mean of 1996 and 1997), respectively.

may be on a trajectory of increasing net carbon uptake as the canopy develops over the next several decades, while the old forest may be on a trajectory of a gradual decline. At both sites, model results show that disturbance history is a more important determinant of current NEP than either interannual climate variability or changing CO_2 concentration. There are important interactions between increasing CO_2, disturbance history and interannual climate variability, which increase in magnitude as CO_2 concentration rises. Fine root : leaf allocation dynamics appear to exert a strong control on NEP response in the decades following a stand-replacing

disturbance. Long-term measurements would be useful for understanding changes in NEP with developmental stage, and time since disturbance.

Acknowledgements

This study was funded by NASA (grant no. NAG5-7531), and DOE (grant no. FG0300ER63014). P.E. Thornton was supported by NASA (grant no. NAS5-31368) and NSF (grant no. DEB-9977066). We gratefully acknowledge Darrin Moore for his field assistance, Chris Andersen for his minirhizotron estimates of fine root turnover rates, and Mark Harmon for the use of his Monte Carlo model. We appreciate the Sisters Ranger District of the US Forest Service for allowing us to conduct research at the old forest, which is in a Research Natural Area, and Willamette Industries for allowing us to conduct research at the young site.

References

Anthoni PM, Law BE, Unsworth MH (1999) Carbon and water vapor exchange of an open-canopied ponderosa pine ecosystem. *Agricultural and Forest Meteorology*, **95**, 115–168.

Auble DL, Meyers TP (1992) An open path, fast response infrared absorption gas analyzer for H_2O and CO_2. *Boundary Layer Meteorology*, **59**, 243–256.

Chen JM (1996) Optically-based methods for measuring seasonal variation of leaf area index in boreal conifer stands. *Agricultural and Forest Meteorology*, **80**, 135–163.

Cohen WB, Harmon ME, Wallin DO, Fiorella M (1996) Two decades of carbon flux from forests of the Pacific Northwest. *Bioscience*, **46**, 836–844.

Comeau PG, Kimmins JP (1989) Above- and bleowground biomass and production of lodgepole pine on sites with differing moisture regimes. *Canadian Journal of Forest Research*, **19**, 447–454.

De Pury GGD, Farquhar GD (1997) Simple scaling of photosynthesis from leaves to canopies without the errors of big-leaf models. *Plant, Cell and Environment*, **20**, 537–557.

DeFries RS, Field CB, Fung I, Collatz GJ, Bounoua L (1999) Combining satellite and biogeochemical models to estimate global effects of human-induced land cover change on carbon emissions and primary production. *Global Biogeochemical Cycles*, **13**, 803–815.

Gholz HL (1982) Environmental limits on aboveground net primary production, leaf area, and biomass in vegetation zones of the Pacific Northwest. *Ecology*, **63**, 469–481.

Gholz HL, Wedin DA, Smitherman SM, Harmon ME, Parton WJ (2000) Long-term dynamics of pine and hardwood litter in contrasting environments: toward a global model of decomposition. *Global Change Biology*, **6**, 1–15.

Giardina CP, Ryan MG (2001) Total belowground carbon allocation in a fast growing Eucalyptus plantation estimated using a carbon balance approach. *Ecosystems*, in press.

Goulden ML, Munger JW, Fan S-M, Daube BC, Wofsy SC (1996) Measurements of carbon sequestration by long-term eddy covariance: methods and a critical evaluation of accuracy. *Global Change Biology*, **2**, 169–182.

Gower ST, Gholz HL, Nakane K, Galdwin VC (1994) Production and carbon allocation patterns of pine forests. *Ecological Bulletins*, **43**, 115–135.

Gower ST, Vogel JG, Norman JM, Kucharik CJ, Steele SJ, Stow TK (1997) Carbon distribution and aboveground net primary production in aspen, jack pine, and black spruce stands in Saskatchewan and Manitoba, Canada. *Journal of Geophysical Research*, **102**, 29, 029–29, 043.

Grier CC, Logan RS (1977) Old-growth *Pseudotsuga menziesii* communities of a western Oregon watershed: biomass distribution and production budgets. *Ecological Monographs*, **47**, 373–400.

Grier CC, Vogt KA, Keyes MR, Edmonds RL (1981) Biomass distribution and above- and below-ground production in young and mature *Abies amabilis* zone ecosystems of the Washington Cascades. *Canadian Journal of Forest Research*, **11**, 155–167.

Harmon ME, Bible K, Ryan MJ, Shaw D, Chen H, Klopatek J, Li X (2001) Production, respiration, and overall carbon balance in an old-growth *Pseudotsuga/Tsuga* forest ecosystem. *Ecosystems*, in press.

Harmon ME, Ferrell WK, Franklin JF (1990) Effects on carbon storage of conversion of old-growth forests to young forests. *Science*, **247**, 699–702.

Harmon ME, Sexton J (1996) *Guidelines for Measurements of Woody Detritus in Forest Ecosystems.* Publication no. 20. U.S. LTER Network Office. University of Washington, Seattle, WA.

Hoover CM, Birdsey RA, Heath LS, Stout SL (2000) How to estimate carbon sequestration on small forest tracts. *Journal of Forestry*, **98**, 13–19.

Houghton RA, Hackler JL, Lawrence KT (1999) The U.S. carbon budget: contributions from land-use change. *Science*, **285**, 574–578.

Irvine J, Law BE (2001) Water limitations to carbon exchange in old-growth and young ponderosa pine stands. *Tree Physiology*, in press:

Keane RE, Ryan KC, Running SW (1996) Simulating effects of fire on northern Rocky Mountain landscapes with the ecological process model FIRE-BGC. *Tree Physiology*, **16**, 319–331.

Kimball JS, White MA, Running SW (1997) BIOME-BGC simulations of stand hydrologic processes for BOREAS. *Journal of Geophysical Research*, **102**, 29, 043–29, 052.

Law BE, Baldocchi DD, Anthoni PM (1999b) Below-canopy and soil CO_2 fluxes in a ponderosa pine forest. *Agricultural and Forest Meteorology*, **94**, 13–30.

Law BE, Cescatti A, Baldocchi DD (2001a) Leaf area distribution and radiative transfer in open-canopy forests: Implications to mass and energy exchange. *Tree Physiology*, **21**, 777–787.

Law BE, Ryan MG, Anthoni PM (1999a) Seasonal and annual respiration of a ponderosa pine ecosystem. *Global Change Biology*, **5**, 169–182.

Law BE, Van Tuyl S, Cescatti A, Baldocchi DD (2001b) Estimation of leaf area index in open-canopy ponderosa pine forests at different successional stages and management regimes in Oregon. *Agricultural and Forest Meteorology*, **108**, 1–14.

Law BE, Waring RH, Anthoni PM, Aber JD (2000a) Measurement of gross and net ecosystem productivity and water vapor exchange of a *Pinus ponderosa* ecosystem, and an evaluation of two generalized models. *Global Change Biology*, **6**, 155–168.

Law BE, Williams M, Anthoni PM, Baldocchi DD, Unsworth MH (2000b) Measuring and modeling seasonal variation of carbon

dioxide and water vapor exchange of a *Pinus ponderosa* forest subject to soil water deficit. *Global Change Biology*, **6**, 613–630.

Monleon VJ, Cromack K, Landsberg J (1997) Short and long-term effects of prescribed underburning on nitrogen availability in ponderosa pine stands in Central Oregon. *Canadian Journal of Forest Research*, **27**, 369–378.

Murray BC, Prisley SP, Birdsey RA, Sampson RN (2000) Carbon sinks in the Kyoto protocol: potential relevance for U.S. forests. *Journal of Forestry*, **98**, 6–11.

Post WM, Kwon KC (2000) Soil carbon sequestration and land-use change: processes and potential. *Global Change Biology*, **6**, 317–328.

Powell DS, Faulkner JL, Darr DR, Zhu Z, MacCleery DW (1993) Forest resources of the United States, 1992. *GTR RM-234*, pp. 44–50. USDA Rocky Mountain Forest and Range Experiment Station, Fort Collins, CO.

Ross DW, Walstad JD (1986) Estimating aboveground biomass of shrubs and young ponderosa and lodgepole pines in southcentral Oregon. *Research Bulletin 57*, Forest Research Lab, Oregon State University, Corvallis, OR.

Runyon J, Waring RH, Goward SN, Welles JM (1994) Environmental limits on net primary production and light-use efficiency across the Oregon transect. *Ecological Applications*, **4**, 226–237.

Ryan MG (1991) A simple method for estimating gross carbon budgets for vegetation in forest ecosystems. *Tree Physiology*, **9**, 255–266.

Ryan MG, Bond BJ, Law BE, Hubbard RM, Woodruff D, Cienciala E, Kucera J (2000) Transpiration and whole-tree conductance in ponderosa pine trees of different heights. *Oecologia*, **124**, 553–560.

Schimel DS, Enting I, Heimann M, Wigley TML, Raynaud D, Alves D, Siegenthaler U (1994) CO_2 and the carbon cycle. In: *Climate Change 1994. Radiative Forcing of Climate Change* (eds Houghton JT *et al.*), pp. 39–71. IPCC Report. Cambridge University Press, Cambridge, UK.

Schimel D, Melillo J, Tian H, McGuire AD, Kicklighter D, Kittel T, Rosenbloom N, Running S, Thornton P, Ojima D, Parton W, Kelly R, Sykes M, Nielson R, Rizzo B (2000) Contribution of increasing CO2 and climate to carbon storage by ecosystems in the United States. *Science*, **287**, 2004–2006.

Schlesinger WH (1985) Changes in soil carbon storage and associated properties with disturbance and recovery. In: *The Changing Carbon Cycle: a Global Analysis* (eds Trabalka JR, Reichle DE). Springer, New York.

Scholander PE, Hammel HT, Bradstree ED, Hemmingsen EA (1965) Sap pressure in vascular plants. *Science*, **148**, 339–346.

Schotanus PH, Nieuwstadt FTM, de Bruin HAR (1983) Temperature measurements with a sonic anemometer and its application to heat and moisture fluxes. *Boundary-Layer Meteorology*, **26**, 81–93.

Schulze E-D, Lloyd J, Kelliher FM, Wirth C, Rebmann C, Luhker B, Mund M, Knohl A, Milyukova M, Schulze W, Dore S, Grigoriev S, Kolle O, Panfyorov MI, Tchebakova N, Vygodskaya NN (1999) Productivity of forests in the Eurosiberian boreal region and their potential to act as a carbon sink – a synthesis. *Global Change Biology*, **5**, 703–722.

Schulze E-D, Wirth C, Heimann M (2000) Managing forests after Kyoto. *Science*, **289**, 2058–2059.

Thornton PE (1998) Regional ecosystem simulation: combining surface- and satellite-based observations to study linkages between terrestrial energy and mass budgets. PhD Thesis, The University of Montana, Missoula.

Thornton PE, Hasenauer H, White MA (2001) Simultaneous estimation of daily solar radiation and humidity from observed temperature and precipitation: an application over complex terrain in Austria. *Agricultural and Forest Meteorology*, **104**, 255–271.

Thornton PE, Running SW (1999) An improved algorithm for estimating incident daily solar radiation from measurements of temperature, humidity, and precipitation. *Agricultural and Forest Meteorology*, **93**, 211–228.

Thornton PE, Running SW, White MA (1997) Generating surfaces of daily meteorological variables over large regions of complex terrain. *Journal of Hydrology*, **190**, 214–251.

USDA (1965) *Silvics of Forest Trees of the United States*. Agriculture Handbook no. 271. U.S. Department of Agriculture, Washington, DC.

Vogt KA, Grier CC, Vogt DJ (1986) Production, turnover, and nutrient dynamics of above- and belowground detritus of world forests. *Advances in Ecological Research*, **15**, 303–377.

Waring RH, Running SW (1998) *Forest Ecosystems – Analysis at Multiple Scales*. Academic Press, San Diego, CA.

Webb EK, Pearman GI, Leuning R (1980) Correction of flux measurements for density effects due to heat and water vapour transfer. *Quarterly Journal of the Royal Meteorological Society*, **106**, 85–100.

Williams M, Law BE, Anthoni PM, Unsworth MH (2000) Carbon–water interactions in ponderosa pine ecosystems. *Tree Physiology*, **21**, 287–298.

Yatskov MA (2000) A chronosequence of wood decomposition in the boreal forests of Russia. MS Thesis. Oregon State University, Corvallis, OR, USA.